http://dx.doi.org/10.1097/mm9.0000000000000040

MedMat

Review

OPEN

Thermoelectric materials for skin wound healing

Ying Zhang[a], Zhining Hao[a], Zhou Li[b,c], Yiping Mu[d], Zhaoxu Meng[a,*], He Lian[a,*]

Abstract

Skin wound healing remains a significant clinical challenge, with traditional therapies often facing issues such as infection and secondary trauma. Thermoelectric (TE) materials possess the unique ability to convert thermal energy into electrical energy. Electrical signals generated by these materials can accelerate skin wound healing by reconstructing endogenous electric fields, modulating the inflammatory microenvironment, and promoting angiogenesis. Despite their substantial potential, a comprehensive understanding of the mechanisms, biocompatibility, antimicrobial properties, and practical applications of TE materials in skin wound healing is still lacking. This review aims to highlight recent advancements in wound healing using TE materials, while integrating considerations of flexibility, biocompatibility, and antimicrobial performance to optimize TE device design. Strategies for enhancing TE performance, such as carrier concentration modulation, band engineering, and lattice thermal conductivity reduction, are discussed to balance conductivity and the Seebeck coefficient. Although challenges in biosafety and room-temperature performance regulation of inorganic materials persist, future developments in multimodal synergistic therapy, intelligent monitoring systems, and novel material design are expected to drive the clinical translation of TE materials for treating refractory wounds.

Keywords: Endogenous electric field, Skin wound healing, Thermoelectric devices, Thermoelectric materials

1. Introduction

The skin, as the body's largest organ, is highly vulnerable to damage and plays critical roles in thermal regulation, mechanical resistance, and infection defense[1–3]. Trauma often induces abnormal inflammation, insufficient extracellular matrix deposition, reduced angiogenesis, and inadequate growth factor stimulation, all of which significantly delay wound healing[4]. Impaired wound healing can lead to pathogen invasion, severe infections, and even life-threatening conditions[5]. Globally, millions of patients require traumatic wound treatment annually, imposing a substantial economic burden[6]. Conventional approaches, such as antibiotic therapy and conventional dressings (e.g., gauze and cotton), present significant limitations such as drug resistance, wound adhesion, secondary injury during dressing changes, and inadequate infection control[7–9]. Ultrasonic devices are large in size, technically complex, and their mechanism of action has not been fully elucidated. Additionally, high-intensity focused ultrasound may generate shear stress on biological tissues, thereby causing damage[10]. Crucially, traditional electrical stimulation devices also rely on external power sources, highlighting the critical need for innovative self-powered strategies, particularly those leveraging thermoelectric (TE) principles, to enable effective, autonomous wound therapy.

Among numerous self-powered wound treatment strategies, TE materials have been proven to be promising candidates for wound treatment. TE materials offer a promising approach by leveraging the Seebeck, Peltier, and Thomson effects to convert heat and electricity[11–13]. In scenarios such as electric field (EF) generation in biological tissues, the Seebeck effect generates a potential difference via charge carrier diffusion across a temperature gradient (Figure 1A), which is of great significance for wound healing. The Peltier effect enables heat absorption/release at conductor junctions (Figure 1B). Notably, the wound healing process is highly sensitive to local temperature: moderate hypothermia regulation can inhibit inflammatory responses and reduce tissue edema, while traditional cold compress methods struggle to achieve precise and continuous targeted temperature control. Based on the Peltier effect, TE materials can realize efficient cooling and precise temperature regulation by modulating electric current[14], thereby providing a novel approach for local temperature management of wounds. While the Thomson effect describes heat exchange in conductors with temperature gradients and electric currents (Figure 1C)[11,15].

In skin wound treatment, TE materials offer self-powered operation and multimodal regulation. The Seebeck effect generates μA-level currents from body-environment temperature gradients (10 K), mimicking endogenous bioelectricity to activate fibroblast migration and angiogenesis. In addition, TE materials can trigger electron/hole redox reactions, which generate reactive oxygen species (ROS). These ROS mediate oxidative damage that nonselectively attacks the key components of bacterial cells, thereby inhibiting infection and achieving the goal of broad-spectrum antibacterial activity[16,17]. These functions not only address the clinical requirements for high efficiency and therapeutic efficacy of wound dressings but also offer a precision-engineered and sustainable strategy for refractory wounds, such as diabetic ulcers and severe burns.

This review summarizes the current state of the art in TE materials and self-powered TE devices that replicate the thermal and electrical microenvironment for skin wound healing. It highlights TE materials as well as self-powered TE stimulation technologies. First, we discuss the origin and

[a]School of Medical Devices, Shenyang Pharmaceutical University, Shenyang, China, [b]Tsinghua Changgung Hospital, School of Clinical Medicine, Tsinghua University, Beijing, China, [c]School of Biomedical Engineering, Tsinghua University, Beijing, China, [d]Central Hospital Affiliated to Shenyang Medical College, Shenyang, China.

**Corresponding authors: Address: Zhaoxu Meng, School of Medical Devices, Shenyang Pharmaceutical University, Shenyang 110016, China. E-mail address: mengzhaoxu2006@163.com (Z. Meng); He Lian, School of Medical Devices, Shenyang Pharmaceutical University, Shenyang 110016, China. E-mail address: lianhe126@126.com (H. Lian).*

MedMat (2026) 3:2

Received: 30 September 2025; Accepted 19 January 2026

Published online 17 April 2026

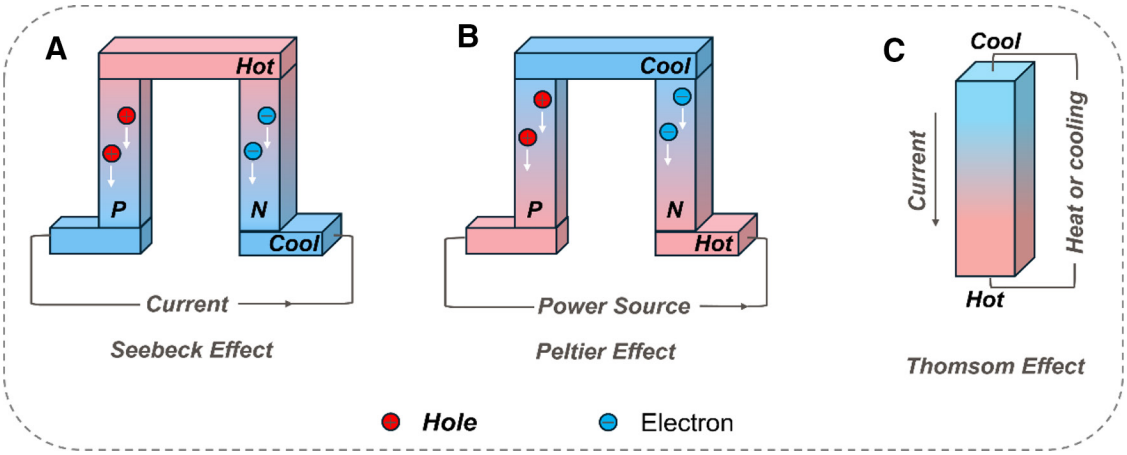

Figure 1. The 3 major thermoelectric effects. (A) Seebeck effect. (B) Peltier effect. (C) Thomson effect.

mechanisms underlying endogenous heat and electrical signals in the skin wound microenvironment. Second, we analyze the design and biocompatibility of TE materials with emphasis on skin wound therapy applications. Finally, we outline performance-enhancement strategies for diverse TE materials in skin wound healing and identify potential obstacles for future clinical translation.

2. Fundamentals of thermoelectric for wound healing

2.1 Classification of thermoelectric materials

Recent studies have logically demonstrated the key role of the Seebeck effect in biomedical applications. From a microscopic perspective, the Seebeck effect originates from the behavior of charge carriers within a material under a temperature gradient. For a single, standalone material, when the temperature inside it is uniform, the distribution of charge carriers is also relatively uniform. Once a temperature difference (ΔT) arises, the charge carriers at the hot end possess higher kinetic energy, so they diffuse toward the cold end and accumulate there. The nonuniform distribution of charge carrier concentration generates a built-in EF inside the material, which induces charge drift motion within the material. The direction of this charge drift motion is opposite to that of the charge diffusion motion driven by the temperature field, thus preventing further diffusion of charge carriers. When these 2 movement tendencies reach equilibrium, there is no net charge flow inside the material, and a stable electric potential U is formed across the 2 ends of the material. The Seebeck coefficient (S) of a single material under a temperature difference (ΔT)can be expressed as:

$$S = \lim_{\Delta T \to 0} \frac{\Delta U}{\Delta T}, \quad (1)$$

For a circuit composed of 2 different materials (A and B), its Seebeck coefficient (S) can be expressed as:

$$S_{AB} = S_A - S_B, \quad (2)$$

To evaluate the energy conversion efficiency of TE materials, the dimensionless figure-of-merit (ZT)[18,19] is defined as:

$$ZT = S^2 \sigma T / \kappa = PF / \kappa, \quad (3)$$

where σ is electrical conductivity, T is absolute temperature, κ is thermal conductivity, and PF is the power factor. The values of S, σ, and T are highly coupled, so decoupling them poses the main challenge in enhancing the performance of the composite material.

TE materials are categorized into n-type and p-type based on their dominant charge carriers, and differences in the dominant mobile charge carriers between these 2 types result in variations in the direction of current flow within the TE materials[20]. The main carriers in n-type TE materials are electrons, whose migration and motion play a key role in the TE properties of the material. Under the action of EF, the electrons can move rapidly and directionally to form an electric current, thus generating the TE effect[21]. It usually has high conductivity, which is favorable for the transport of electrons and can reduce the Joule heat loss, thus improving the TE conversion efficiency of the material. And the absolute value of its Seebeck coefficient is relatively high; a higher Seebeck coefficient means that under the same temperature difference conditions, the material can produce a larger voltage, which is very important for the improvement of TE conversion efficiency. The main carriers in p-type TE materials are holes, whose migration and motion lead to the generation of electric current and the TE effect. The mobility of holes is usually relatively low compared with electrons in n-type TE materials[22]. P-type TE materials generally have positive Seebeck coefficients, which are comparable or slightly lower in absolute value than the Seebeck coefficients of n-type TE materials. In terms of conductivity, p-type TE materials may have a slightly lower conductivity relative to n-type materials[23].

Based on the type of material, they can be categorized into inorganic TE materials, organic TE materials, and their composite materials in Table 1. Inorganic TE materials have better TE properties than organic TE materials. Bismuth telluride (Bi_2Te_3)-based flexible TE devices possess the characteristics of being lightweight, compact in size, and highly deformable. These devices are capable of harvesting electrical energy from temperature gradients, thereby serving as an energy source for wearable devices[32], as shown in Figure 2. Additionally, they can function as miniature TE cooling pads for localized refrigeration applications[34]. Lead telluride-based semiconductors[35], skutterudites[36], and Half-Heusler alloys[37] have the ability to convert thermal energy into electrical energy. These materials can be applied in scenarios such as power generation from industrial waste heat and the recovery of waste heat from automotive exhaust. By doing so, not only is the energy utilization efficiency enhanced, but emissions can also be reduced. Organic TE materials have been widely applied due to their abundant resources, low cost, excellent flexibility, and high biocompatibility[38]. Poly(3,4-ethylenedioxythiophene)-poly (styrenesulfonate) (PEDOT:PSS), characterized by its relatively high electrical conductivity and excellent flexibility, is one of the organic TE polymer materials that have been extensively

Table 1

Comparison of thermoelectric material properties (Tested at a temperature of 300K.).

Thermoelectric materials	σ(S/m)	S(μV/K)	PF(μW/m·K²)	κ(W/m·K)	ZT	References
Inorganic materials						
Bi_2Te_3	690	−177.2	2170	/	/	[24,25]
Ag_2Se	497	−140	987.4	0.478	0.6	[24,26]
Organic materials						
PEDOT: PSS	1831	28	144	0.29	0.11	[27,28]
PANI	1241	51.3	34.74	0.321	0.325	[29]
Inorganic/organic hybrids						
Bi_2Te_3/PEDOT:PSS	1350	49	324	0.3	0.28 ± 0.04	[30]
PEDOT:PSS/$Bi_{0.5}Sb_{1.5}Te_3$	1285	49	308	0.2	0.484	[31]

PANI, polyaniline; PF, power factor.

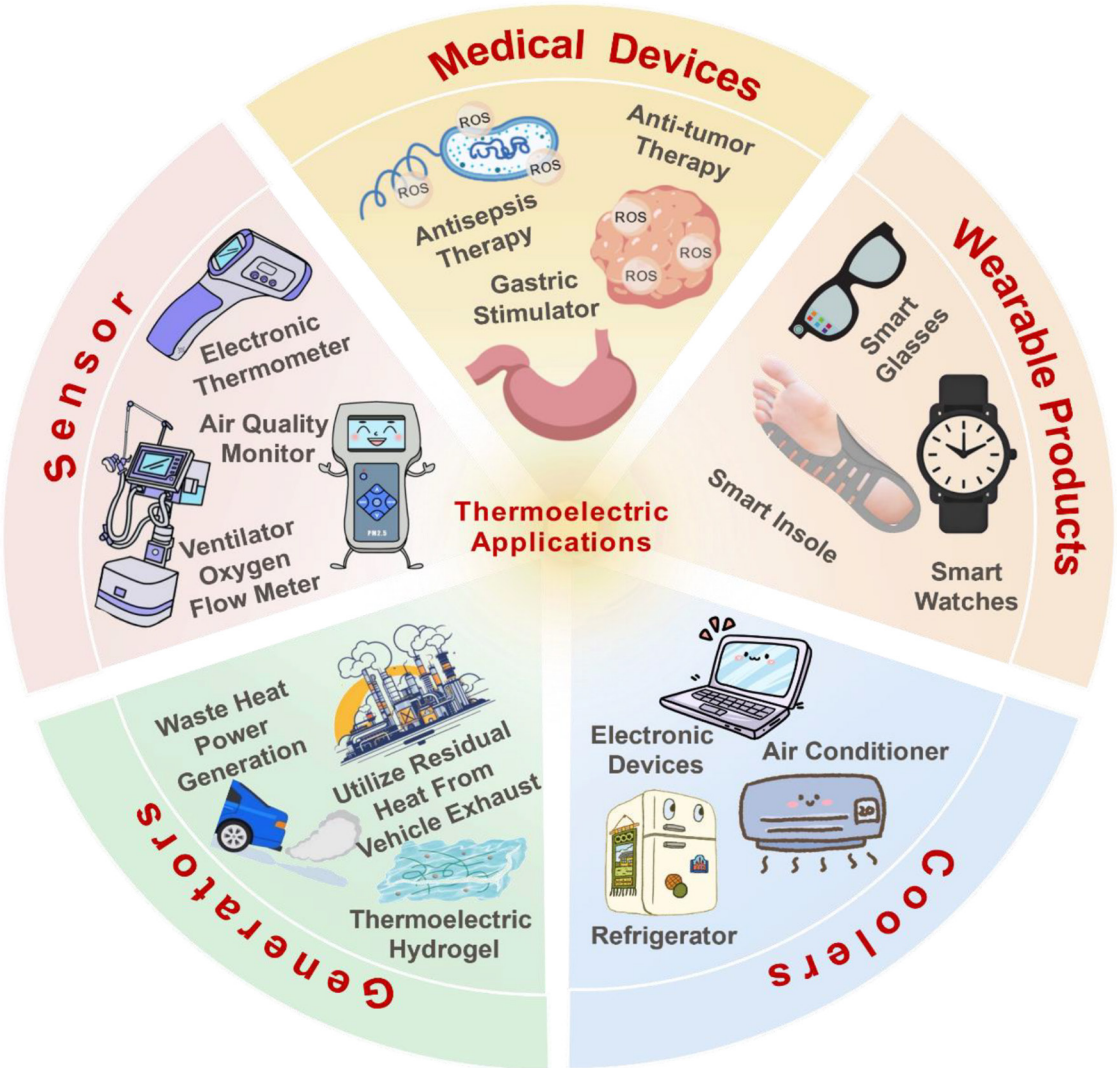

Figure 2. The applications of thermoelectric materials in various fields. (Created with BioGDP.com[33]).

investigated and demonstrate outstanding performance. It holds potential application values in fields such as flexible TE devices[39] and wearable electronic devices[40]. Polyaniline (PANI) exhibits excellent electrical conductivity and a notable TE effect. It can be prepared through simple processes such as the solution method, and its relatively low production cost makes it advantageous[41]. PANI is applicable for the fabrication of various materials and devices, including biosensors and electrode materials. Composite materials integrate the respective advantages of organic and inorganic materials. To a certain extent, they can achieve a synergistic enhancement of electrical conductivity and the Seebeck coefficient, thereby improving the TE properties of the materials, which is manifested as an increase in the power factor (PF). Consequently, this leads to an improvement in the TE conversion efficiency[42]. Some TE materials have been applied in the medical field, such as Bi_2Te_3, PEDOT:PSS, and others; while other TE materials are expected to be further extended to multiple research and application directions in the

biomedical field through systematic performance-enhancement strategies, such as rational material design, optimization, or the doping of other substances.

2.2 Interaction mechanisms of thermoelectric materials with skin wounds

TE materials exploit the Seebeck effect to directly convert the small temperature gradient between a skin wound and the surrounding environment into a microcurrent, forming the physical basis for the electrical signal interaction between the device and the wound. When a temperature gradient exists across the material, charge carriers diffuse from the high-temperature side (wound) to the low-temperature side (environment), generating a potential gradient whose magnitude depends on both the material's Seebeck coefficient and the temperature gradient[43]. Enhancing conversion efficiency requires materials with a high Seebeck coefficient and optimized interfacial thermal resistance[42]. Crucially, this process does not require an external power source, achieving a self-powering operation that provides a solid foundation for continuous treatment.

As shown in Figure 3A, normal epithelial tissue establishes a transepithelial potential (≈10–60 mV) through sodium, potassium, and chloride ion transport (Na^+, K^+, Cl^-)[44]. Following epithelial disruption, ion pumps in epithelial cells generate an extracellular EF, termed the endogenous EF (≈40–200 mV/mm, directed from wound edge to center) in Figure 3B and C[45]. Chronic wounds exhibit persistent inflammation and excessive matrix degradation, reducing endogenous EF strength and impairing fibroblast migration;[16] electrolyte loss at the wound site further attenuates the endogenous EF, hindering cell migration/proliferation and significantly impeding skin regeneration[46]. Consequently, EF modulation represents a promising therapeutic strategy. When a temperature differential (ΔT = 10 K, simulating body-environment variance) is applied, the TE material generates a microcurrent (5–35 μA/cm^2) that reconstructs the impaired endogenous EF—rendering wound-site field intensity approximately physiological—while directing cell adhesion and migration toward the wound center[47]. This process simulates physiological electrical signals, compensates for the endogenous EF deficiency in chronic wounds, and activates electrophysiological behavior in injured cells/tissues to achieve treatment.

The inflammatory response in skin wound healing manifests phased characteristics[48]. The acute inflammatory phase commences with the release of histamine by mast cells. Neutrophils infiltrate rapidly and peak within 24 hours. The concentration of the pro-inflammatory cytokine tumor necrosis factor-α surges promptly, facilitating the clearance of pathogens and necrotic tissues[49]. If inflammation fails to resolve in a timely fashion, the transition to the chronic inflammatory phase occurs. During this stage, M1-type macrophages constitute over 70% of the cell population, continuously secreting the pro-inflammatory cytokine IL-6. Concurrently, the activity of matrix metalloproteinase-9 escalates by a factor of 3 to 5, culminating in the over-degradation of the extracellular matrix[50]. This phase is accompanied by pronounced oxidative stress, with the level of ROS being tens of times higher than that in normal tissues[51]. Consequently, protein carbonylation modification increases by 40%, further inhibiting the repair process[52]. In physiological wound healing, the concentration of vascular endothelial growth factor (VEGF) peaks at 72 hours after injury, driving sprouting angiogenesis. Nevertheless, in chronic wounds, the expression of VEGF diminishes by 40%[53]. Simultaneously, there is a disruption in the balance of vascular stabilization signals, thereby establishing a repair-destruction vicious cycle, which ultimately obstructs reepithelialization and functional restoration. Electrical signals trigger multidimensional repair effects by activating related signaling pathways. As shown in Figure 4, the EF generated by silver selenide (Ag_2Se) notably downregulates the expression of prolyl hydroxylase 2, thereby enhancing the stability of hypoxia-inducible factor-1α (HIF-1α) and preventing its ubiquitin-mediated degradation. As a transcription factor, HIF-1α promotes the expression of VEGF-A, a key mediator of angiogenesis that facilitates endothelial cell proliferation, migration, and vessel formation[54]. Furthermore, Qin's study indicates that the electrical signals generated by Ag_2Se activate voltage-gated calcium channels on the cell membrane, thereby increasing intracellular Ca^{2+} concentration. Ca^{2+} activates calmodulin-dependent kinase β, which in turn phosphorylates adenosine monophosphate-activated protein kinase. This phosphorylation event subsequently triggers the activation of the nuclear factor-erythroid 2 related

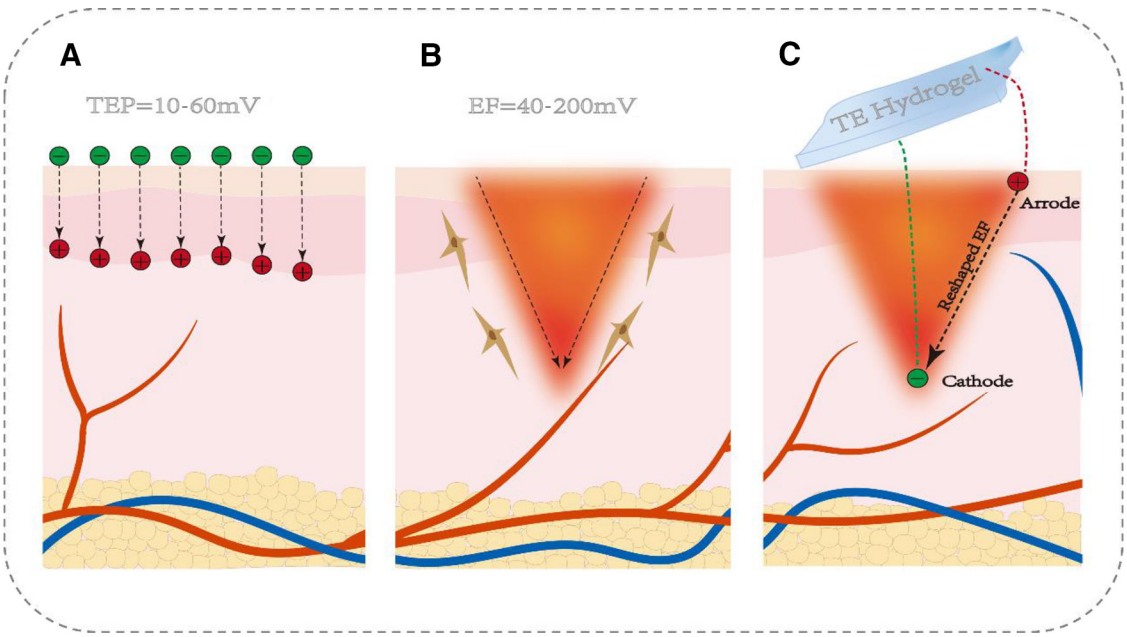

Figure 3. Schematic illustration for therapeutic program thermoelectric devices. (A) transepithelial potential. (B) Endogenous electric field. (C) Reshape endogenous electric field.

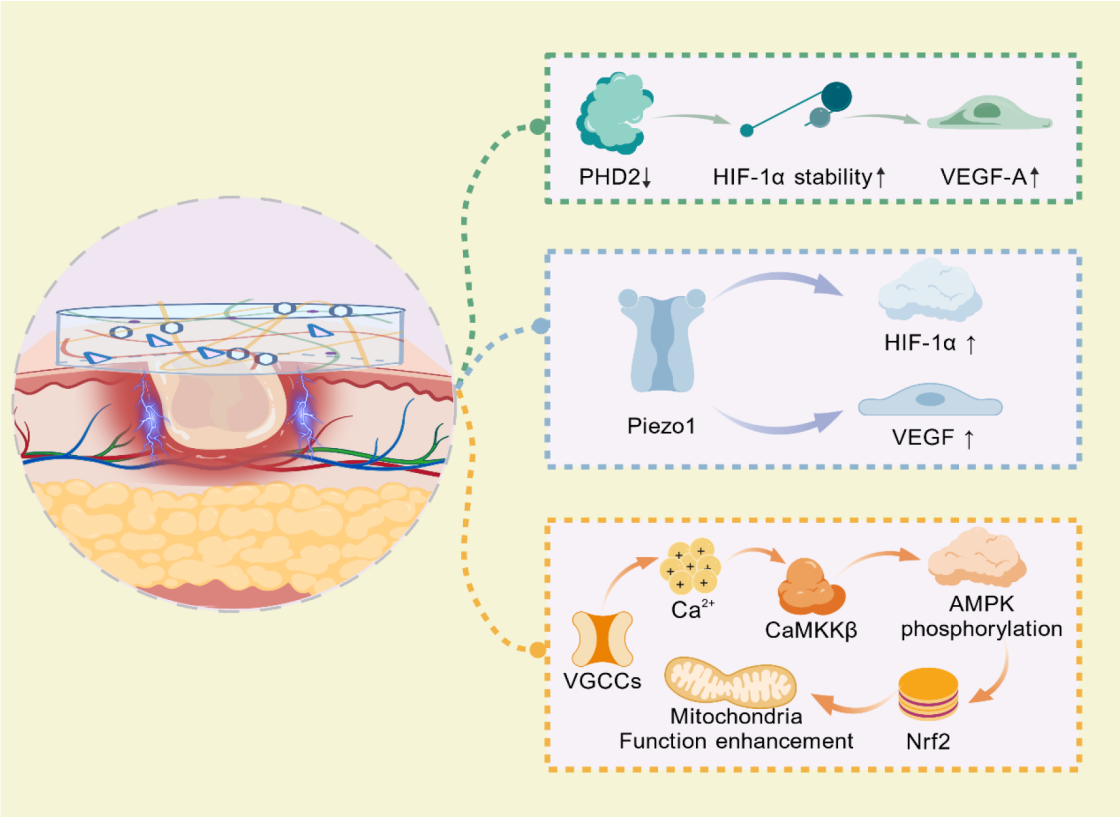

Figure 4. Thermoelectric materials and skin wounds interaction with electrical signals. (Created with BioGDP.com[33]).

factor 2, enhancing mitochondrial function while improving mitochondrial dynamics. Collectively, these cascades promote endothelial cell proliferation and tube formation, accelerate fibroblast migration, and facilitate angiogenesis and tissue regeneration[55]. The TE device fabricated by Zhang et al.[56] that not only promotes wound healing but also demonstrates that the microvolt-level electrical signals it generates activate the mechanosensitive ion channel Piezo1. The microvolt-level electrical signals generated by TE materials can also activate the mechanosensitive ion channel Piezo1. Piezo1, in turn, upregulates the expression of HIF-1α and VEGF, thereby enhancing fibroblast migration and proliferation as well as endothelial tube formation[56]. Numerous studies have demonstrated that endogenous EF at wound sites is attenuated due to electrolyte loss. Leveraging the temperature difference between the wound and the surrounding environment to generate a continuous compensatory EF restores the impaired endogenous EF. The EF directs the directional migration of keratinocytes and fibroblasts via ion directional migration induced by the Soret effect, while modulating cell proliferation and adhesion[16,57,58]. These pathways are centered on the simulation and restoration of endogenous EFs via electrical signals, which precisely regulate 3 key wound healing processes: fibroblast migration, fibroblast proliferation, and accelerated angiogenesis. Accordingly, aiding epithelial regeneration and matrix remodeling through material design has emerged as a cutting-edge research focus in the fields of biomaterials and regenerative medicine.

3. Thermoelectric dressings for wound healing

Owing to discoveries in bioelectricity and thermoelectricity, TE materials capable of simulating the electrophysiological microenvironment have drawn significant attention due to their ability to replicate endogenous EFs with high biocompatibility and low cost. Substantial efforts have been directed toward designing and fabricating TE materials. By adjusting the composition, topography, and structure, TE material properties can be precisely customized to meet application requirements across diverse pathological conditions and maximize their potential value in skin tissue engineering.

Given the varied structures and properties of TE materials and their applications across skin repair scenarios, designing TE devices for wound treatment necessitates consideration of antibacterial performance, dynamic adhesiveness, and biological safety. In recent years, propelled by the cross-disciplinary integration of flexible electronics, nanotechnology, and artificial intelligence, design strategies for such devices have undergone multidimensional innovation. Subsequent sections elaborate on these strategies, focusing on 3 key aspects: flexible design, biocompatibility, and antimicrobial capacity.

3.1 Flexibility for thermoelectric wound dressing

TE materials and devices are crucial in wearable technology for converting body heat into usable electrical energy to treat skin wounds. However, they must adapt to the complex deformations of human skin. During daily activities, the skin undergoes movements, including joint flexion/extension, muscle contraction, and changes from wound swelling or inflammation[59]. Flexible design is therefore paramount for effective integration into wearable systems, ensuring functionality maintenance while accommodating natural body motion and contours.

In wound dressing applications, hydrogels, owing to their 3-dimensional (3D) structure with a large number of pores inside (Figure 5A), not only enhance physical adsorption but also facilitate permeation of water, nutrients, and bioactive molecules, imparting excellent permeability[60]. This characteristic is vital for wound healing and showcases significant application potential. Notably, Figure 5B–D demonstrates that hydrogels also exhibit exceptional flexibility[61,63]. Hydrogels exhibit

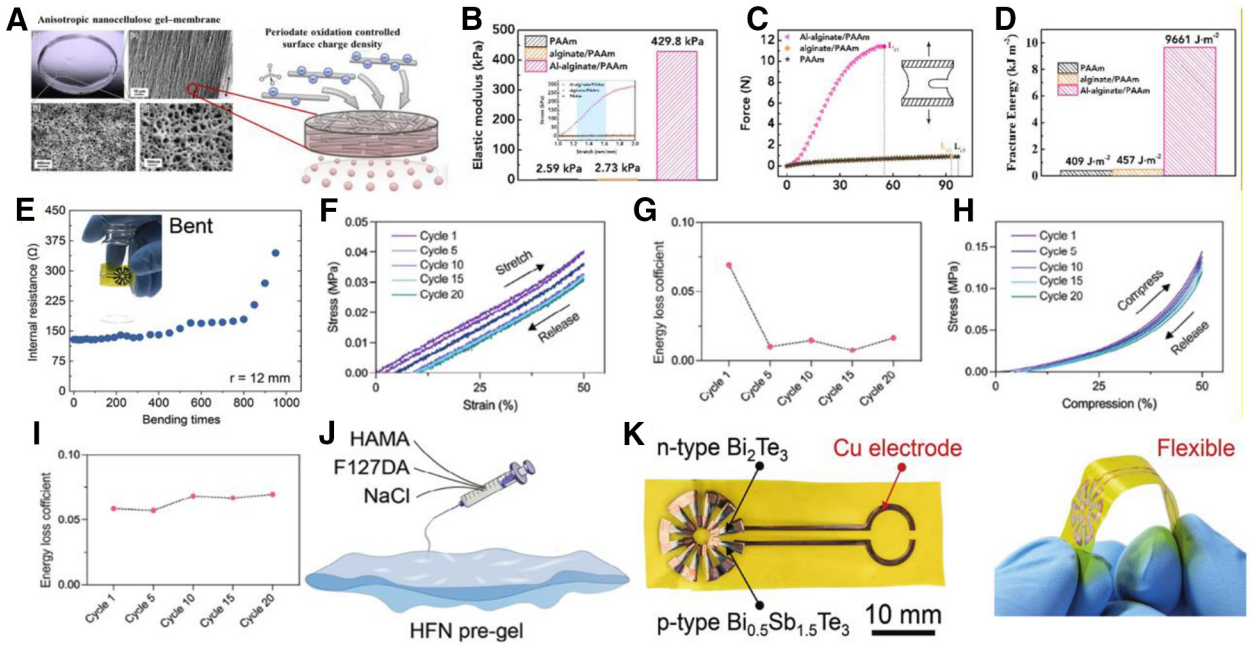

Figure 5. The flexibility of wound dressings. (A) Biocompatibility of thermoelectric materials. The mechanism of drug release from hydrogels[60]. Copyright 2020, Elsevier. (B–D) Tensile modulus, force-length, and fracture energy of hydrogels with different content[61]. Copyright 2019, Elsevier. (E) The internal resistance of the device with respect to the bending times at a bending radius of 12 mm shows that the device negligibly degrades after bending 400 times[62]. Copyright 2025, Wiley-VCH GmbH. (F, G) Stress-strain curves. (F), and hysteresis ratio. (G) During 20 cyclic stretching (H, I) Compress-strain curves. (H), and hysteresis ratio. (I) during 20 cyclic compressions. (J) Schematic illustration of HFN hydrogel construction and thermo-EF generation[56]. Copyright 2024, Wiley-VCH GmbH. (K) Schematic diagram of flexible thermoelectric device structure and flexibility[62]. Copyright 2025, Wiley-VCH GmbH.

remarkable stretchability and elasticity, enabling deformation synchronized with skin movement to ensure continuous contact with the wound. Regardless of joint articulation or bodily motion, hydrogel dressings conform without detaching or tearing during skin stretching/flexion. This flexibility significantly enhances patient comfort—preventing dressing-induced secondary trauma—while crucially maintaining a stable wound microenvironment to facilitate healing. Furthermore, hydrogels' inherent flexibility allows fabrication into diverse shapes/sizes, enabling customization for specific wound characteristics to meet varied clinical needs[64]. In recent years, hydrogel materials, owing to their distinctive properties, particularly the TE behavior, have been replicating the inherent EF[65]. This endeavor has propelled the research, development, and evolution of TE hydrogels. Figure 5J depicts Tan et al.[64] synthesized a TE hydrogel with excellent flexibility, which achieves the simulation of the endogenous EF by virtue of material design and temperature difference-driven mechanisms, thereby addressing the problem of EF deficiency caused by electrolyte loss in diabetic ulcers. The monomer polyether F127 incorporated in this hydrogel demonstrates remarkable stretchability, endowing it with the capacity to modulate the mechanical properties of the hydrogel system. Evident from the research findings, a wireless thermoelectric hydrogel embedded with therapeutic exosomes (HFN-RGE) exhibits a maximum tensile strain surpassing 200% and a maximum compressive strain of around 81% in Figure 5F, G, allowing it to adapt proficiently to the deformations of the human body surface. Moreover, under a 25% tensile or compressive strain, its Young's modulus measures 68.10 KPa and 129.55 KPa, respectively. Figure 5H, I shows that even following 20 cycles of 50% tensile or compressive strain, the hydrogel is capable of completely reverting to its initial state, with the hysteresis ratio consistently maintaining at a relatively low value below 0.1. These inherent characteristics empower the device to adapt with flexibility to diverse movements and deformations of the skin during its practical application[62]. This research provides a guiding example for the future treatment of diabetic ulcers.

In wound-healing research, beyond hydrogels, the emergence of TE devices fabricated from conventional TE materials represents a promising alternative for accelerating wound recovery. These devices utilize temperature gradients to generate electrical energy, delivering microcurrent stimulation to wounds that promotes cell proliferation and migration. Furthermore, their unique material and structural designs offer advantages in adapting to the body's complex physiological environment. For instance, Zhang et al.[56] engineered a circular TE device, thereby ushering in a novel breakthrough in the realm of wound-healing treatment. Figure 5K demonstrates TE structures deposited on a flexible polyimide (PI) substrate via magnetron sputtering. These structures utilize the natural temperature difference between the skin and the environment (6–30 K achievable in daily life) to spontaneously generate electrical energy, and deliver an output voltage of 10 mV under a temperature difference of 10 K, without the need for an external power supply. The left panel shows the circular-shaped multi-leg TE device, consisting of 6 pairs of n-type Bi_2Te_3 and p-type $Bi_{0.5}Sb_{1.5}Te_3$ rectangular thin layers, is sealed by a flexible PI layer. The black and red arrows mark the TE materials and Cu electrode, respectively. The right panel illustrates that this device is extraordinarily flexible, and it can be folded manually. As shown in Figure 5E, under a bending radius of 12 mm, following 400 bending cycles, its internal resistance experiences a negligible decrease. This phenomenon attests to its stable performance postrepeated bending and implies a protracted service life, endowing it with the ability to accommodate the deformation of the skin during locomotion. In terms of its structural configuration, the implementation of a circular design enables it to conform intimately to the skin surface and adapt to wounds located on diverse body regions, thus exemplifying commendable flexibility and tensile capabilities[56].

Although progress has been made in the TE wound therapy devices, significant challenges must be overcome to achieve widespread clinical adoption and market penetration. At the structural design level, current devices lack adequate thinness and fit, necessitating innovative breakthroughs to develop thinner,

lighter, and better-fitting device configurations. Through the use of advanced manufacturing technologies such as 3D printing and personalized customization based on the shape, size, and location of different wounds, it is possible to achieve a close fit between the device and the wound, which significantly improves the therapeutic effect[66]. At the same time, the development of stretchable and foldable structures is the key to adapting the device to the movements and deformations of various parts of the body. Ensuring that the device can cope with complex scenarios, such as joint wound treatment, without affecting its TE properties will ensure that the device continues to work stably[67]. Wu et al.'s study demonstrated that $Ag_2Te_{1-}XSX$ ($0.3 \leq X \leq 0.6$) achieves an ultrahigh elongation of up to 10150% via the mechanism of "anionic sublattice amorphization and Ag^+ ion diffusion." Notably, it can trigger plastic strain with only low stress without structural collapse. Meanwhile, its intrinsic superionic conductivity and plasticity exhibit a synergistic effect: during deformation, the rigid anionic sublattice transforms into a metastable amorphous phase while maintaining local bonding integrity[68]. Their results directly confirm that the designed TE material can conform to irregular wounds, accommodate limb movements, and retain stable TE performance without degradation during deformation. This provides strong support for the selection and design of ideal TE material systems for wound therapy. In terms of clinical application, the safety and efficacy of the device in the treatment of different types of wounds have not yet been adequately studied. In the future, more clinical trials need to be conducted to explore the effectiveness of the device in various wound types and treatment scenarios, and to obtain sufficient clinical data to support and accelerate the product's approval by the regulatory authorities[69]. In addition, reducing the manufacturing cost of the device and improving the production efficiency are equally important directions to promote the large-scale clinical application and market promotion of the device.

3.2 Biocompatibility for thermoelectric wound dressing

Presented in Table 2, TE materials demonstrate unique advantages in wound healing, offering novel therapeutic directions. Ensuring treatment safety and efficacy necessitates an in-depth investigation of TE material-biological tissue interfacial interactions[77]. Biocompatibility, a critical safety criterion for clinical implantation, holds particular significance for these materials, encompassing immediate cell/tissue responses, long-term stability, immune responses, and body fluid compatibility[78].

Comprehensive assessments elucidate the biodegradation behavior of TE materials in vivo, including metabolic pathways and effects on cells, tissues, and organs, as characterized in Figure 6E[83,84]. This, in turn, provides a key basis for its rational design and optimization. In the evaluation process, in vitro and in vivo test methods should strictly follow internationally recognized standards and norms, such as the ISO 10,993 series of standards[85].

A systematic biocompatibility assessment is therefore essential to ensure the safe and effective use of TE materials in biological systems. Gao et al.[24], conducted a comprehensive in vitro and in vivo biocompatibility assessment of 12 typical sulfur compound TE materials, and determined that Ag_2Se, Bi_2Se_3, and Bi_2Te_3 have good biocompatibility, which provides an important basis for their application in the biomedical field. In contrast, materials containing high concentrations of tellurium (Te) ions, such as Te, GeTe, SnTe, MnTe, $Bi_{0.5}Sb_{1.5}Te_3$, and Sb_2Te_3, which have a concentration of Te ions higher than 7.2 ppm, high concentrations of Te trigger irreversible oxidative stress, disrupting intracellular tissues and energy homeostasis, and exhibit significant cytotoxicity[24].

Bi_2Te_3-based composite TE materials are known for their very high room-temperature stability, ease of deposition, high electrical conductivity, and low thermal conductivity[86]. The highest known TE ZT value at room temperature (ZT = 1.86 at 300 K)[87]. Therefore, Bi_2Te_3-based materials have been widely used in biomedical applications. Gao et al.[24] made disc-shaped samples of Bi_2Te_3 (10 mm in diameter and 1 mm in thickness) and implanted them subcutaneously in male Sprague-Dawley (SD) rats. Blood samples and tissue samples from vital organs, including liver, kidney, and heart, as well as those near the implantation site, were collected at 3, 7, and 30 days after implantation for a comprehensive study of in vivo biocompatibility. The results of hematological analysis showed that the key blood parameters of the rats, such as red blood cells, white blood cells, and hemoglobin, were all within the normal range, with no significant difference compared with the titanium alloy control group, which indicated that it has less impact on the blood system, suggesting that it has less impact on the organism and has relatively good biocompatibility. Hematoxylin–eosin (H&E) staining of the collected heart, liver, spleen,

Table 2

The biocompatibility, degradability, and properties in wound exudate of thermoelectric materials.

Thermoelectric materials	Biocompatibility (±)	Degradability (±)	Properties in wound exudate	References
Bi_2Ti_3	+	–	Exhibits stability with low Te^{2+} release. Surface modification can further reduce its cytotoxicity.	[24,70]
Ag_2Se	+	+	Released Se^{2+} and Ag^+ exhibit moderate antibacterial activity, modulate metabolomics, and affords metabolic support for wound healing.	[24,71]
Cu_2Se	+	–	Possessing structural and dispersive stability, it is endowed with SOD-like activity to scavenge free radicals in exudate.	[24,72]
Bi_2Se_3	+	–	Commonly utilized in photothermal therapy and bioimaging, with high stability in wound environments.	[73]
SnSe	–	–	Released Sn^{2+} and Se^{2+} can induce cytotoxicity, yet compositing with TiO_2 enhances biocompatibility.	[24,74]
GeTe	–	–	High Te^{2+} release leads to significant cytotoxicity, making it incompatible with wound environments.	[24,75]
Sb_2Te	–	–	Te^{2+} release causes cytotoxicity, precluding its use in biomedical applications.	[24]
PEDOT:PSS	+	+	Possesses excellent flexibility, ideal for flexible device substrates or electrodes, with good stability in wound environments.	[76]
MgAgSb	/	/	Lack of systematic evaluation in terms of biocompatibility and within the wound environment.	/

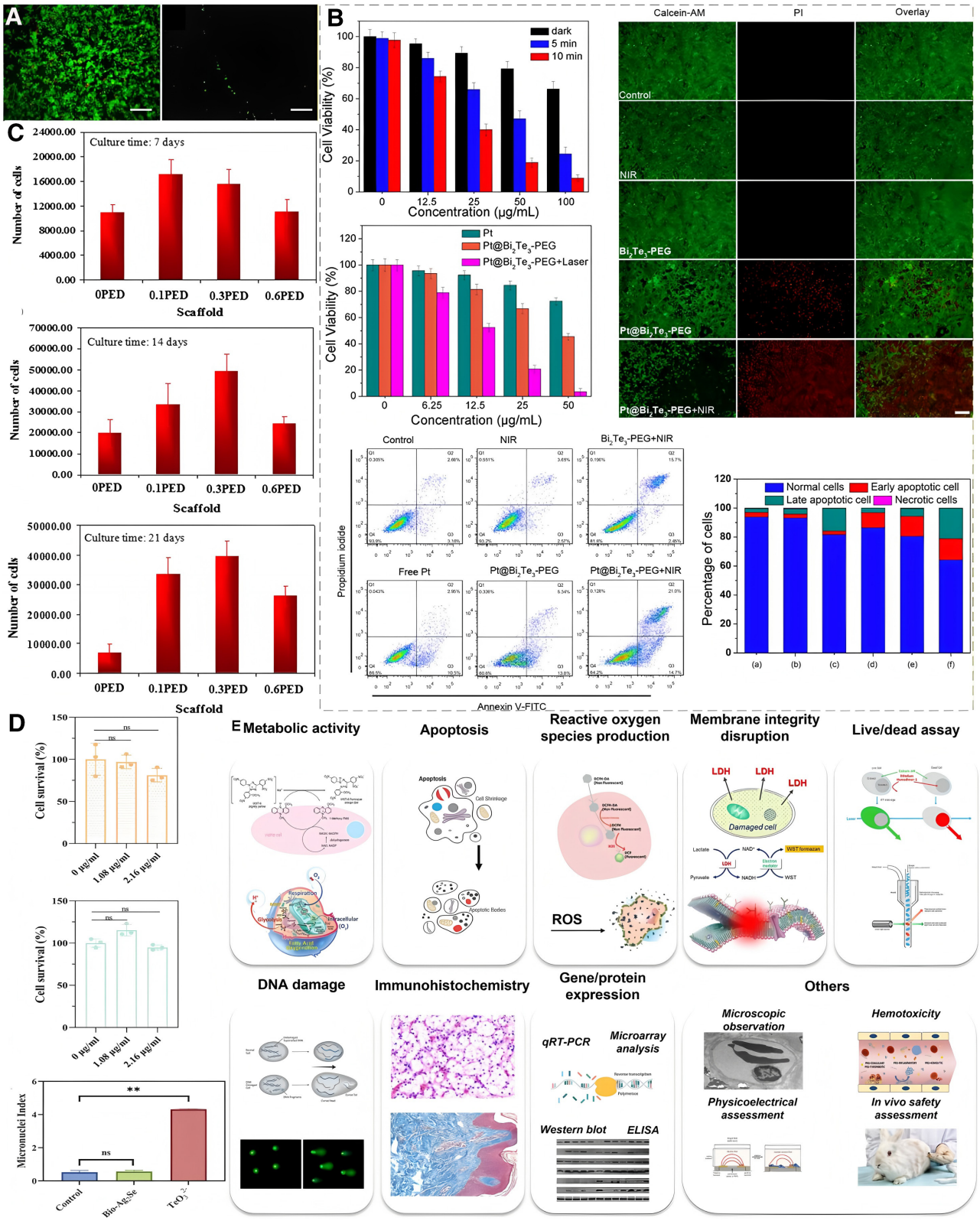

Figure 6. Biocompatibility of thermoelectric materials. (A) Fluorescence live/dead staining of BHK-21 cells cultured on the surfaces of (the left) PI (PI-2525) and (the right) latex rubber (positive control) after 24 hours. Viable cells: green, dead cells: red. Scale bar = 200 μm[79]. Copyright 2009, Elsevier. (B) Cellular biocompatibility of Bi_2Te_3 nanoparticles[80]. Copyright 2020, American Chemical Society. (C) The number of cells after 7, 14, and 21 days of incubation on the 0PED, 0.1PED, 0.3PED, and 0.6PED scaffolds[81]. Copyright 2015, Springer Nature. (D) Cellular biocompatibility of Bio-Ag_2Se nanoparticles[82]. Copyright 2024, Elsevier. (E) Biosafety of inorganic nanomaterials for theranostic application[83]. Copyright 2022, The Moon Sung Kangs.

subcutaneous tissues, and other important organs showed that these organs did not show obvious pathological changes, and the tissue structure remained intact, indicating that the tissues have a relatively good compatibility between Bi_2Te_3 and the surrounding biological tissues[24]. In addition, Ma et al.[80] investigated the biocompatibility of Bi_2Te_3 nanoparticles based on cytotoxicity and hemolysis experiments, and Figure 6B showed that the cell viability of Bi_2Te_3 nanoparticles at different concentrations did not show any significant decrease after 24 hours of incubation in 96-well plates with 4T1 breast cancer cells, which suggests that the composites do not have toxicity effects on cells and have good biocompatibility. This indicates that the composite material does not have toxic effects on cells and has good biocompatibility. Different concentrations (0.125, 0.25, 0.5, 1, and 2 mg/mL) of Bi_2Te_3 nanoparticles were dispersed in PBS, and 0.3 mL of blood was taken and mixed with 1.2 mL of the sample dispersion and incubated for 4 hours at room temperature. The results showed that the hemolysis rate was at a low level, which further proved that the nanoparticles had good biocompatibility and would not cause damage to the blood system, providing stronger support for their application in biomedical fields[80]. Considering the high toxicity of Te elements, when TE devices are in direct contact with the human body, their potential hazards cannot be ignored. Therefore, it is crucial to effectively prevent these harmful substances from coming into contact with the human body. In this case, PI plays an important role, which is the most common flexible substrate material in the field of TE devices, and the staining of the living dead cells in Figure 6A shows that PI is more biocompatible than latex rubber, which avoids any toxicity to the organ[79]. Zhang et al.[56] developed a TE device utilizing Bi_2Te_3-based compounds as the core material. The device demonstrated superior TE performance near room temperature and exhibited robust stability under various environmental conditions. To prevent the possible toxicity of the Te element in the material to living organisms, the device is completely sealed with PI for the entire TE device. This avoids direct contact between the TE material and human tissue and guarantees the biocompatibility of the device at the material level and in the package design[56].

Nevertheless, Te is scarce, expensive in the Earth's crust, and furthermore exhibits potential toxicity, rendering it unsuitable for devices requiring long-term human contact[88]. Moreover, they are also more toxic and not suitable for the preparation of devices that are in long-term contact with the human body. Consequently, developing novel Te-free TE materials has attracted extensive research interest. Ag_2Se, a narrow bandgap n-type semiconductor, exists as a stable orthorhombic phase (β-Ag_2Se) at room temperature (298 K). Its crystalline structure transforms from orthorhombic to cubic (α-Ag_2Se) at approximately 407 K. Notably, β-Ag_2Se exhibits remarkable TE properties at room temperature, with ZT ranging from 0.32 to 1.2[89–95]. Ag_2Se exhibits significantly low toxicity and cost, and its room-temperature TE performance has garnered considerable attention. Gao et al.[24] implanted Ag_2Se subcutaneously into SD rats and monitored at different time intervals for a comprehensive study of its in vivo biocompatibility. H&E staining of the collected organ tissues showed that the heart, liver, spleen, lungs, kidneys, and brain showed no significant pathological changes, and the tissue structure remained intact. This showed that the tissues were well adapted to Ag_2Se, and the material had some compatibility and tissue integration with the surrounding biological tissues. H&E staining and Masson trichrome staining of the subcutaneous tissue at the implantation site showed no signs of macroscopic rupture, infection, necrosis, or edema, reflecting the biocompatibility of the material with the surrounding biological tissues[24]. In addition, Ren et al.[82] synthesized Bio-Ag_2Se nanoparticles as antimicrobial agents from the yeast strain R. mucilaginous PA-1 and evaluated their safety on human and plant cells by cytotoxicity assays. In humans, 293T cells (epithelioid cells) and Jurkat cells (immortalized T-lymphocyte cell line) were selected, and the cells were treated with medium containing 1.08 μg/mL and 2.16 μg/mL of Bio-Ag_2Se nanoparticles, respectively. The assay was performed using cell counting kit-8 reagent, and the relative cell viability was calculated. Figure 6D shows that the relative viability of 293T cells treated for 24 hours was (96.6 ± 8.3)% and (81.2 ± 8.2)% at the concentrations of 1.08 and 2.16 μg/mL, respectively, which was not significantly ($P < 0.05$) different from that of the untreated control group (with a viability of [100 ± 19.0]%). The difference was not significant ($P < 0.05$). The relative viability of Jurkat cells was (115.3 ± 6.9)% and (94.8 ± 3.0)% after 24 h of treatment at the same concentration, respectively, and there was no significant cell death compared with untreated control (viability of [115.3 ± 6.9]%) ($P < 0.05$), and the exposure to Bio-Ag_2Se nanoparticles Jurkat cells respiratory activity slightly increased after exposure to Bio-Ag_2Se nanoparticles[82]. The experimental results show that Bio-Ag_2Se nanoparticles have excellent biocompatibility with human cells and have potential applications in biomedical fields. Quantitative biomarkers are significant for disease diagnosis, health monitoring, and drug development[96–98].

Organic TEs (e.g., PEDOT:PSS) exhibit lower conversion efficiency than inorganic counterparts but offer critical advantages in reduced cytotoxicity and enhanced biocompatibility[99]. PEDOT:PSS shows promise in soft bioelectronics due to its high conductivity and ability to electrically couple with tissues for sensing/stimulation. Yang et al.[100] developed a highly conductive PEDOT:PSS hydrogel demonstrating good biocompatibility with PC12 cells through cytotoxicity testing, live/dead staining, and proliferation experiments, confirming its suitability for in situ cellular sensing. As a biocompatible electrical conductor, its intrinsic conductivity enables stimulation of cultured cells/tissues[101,102]. Mostafa Yazdimamaghani et al.[81] fabricated conductive bone scaffolds incorporating PEDOT:PSS, where Figure 6C shows enhanced cell viability peaking at 0.3%(w/w) concentration. Cells on these scaffolds exhibited extended morphology with filamentous pseudopods connecting to the surface, demonstrating effective adhesion/spreading and forming denser monolayers after 14-day culture, indicating improved scaffold conductivity and biocompatibility[81]. Thus, with controlled concentration and surface modification, PEDOT:PSS is promising for TE therapy applications.

Although numerous strategies[103–106] can enhance the biocompatibility of TE materials, establishing a comprehensive biosafety assessment system remains imperative. This requires unified standards and test methodologies to ensure material/device safety and efficacy. Concurrently, strengthening monitoring and research on the long-term biological effects is essential to generate reliable translational data, thus advancing TE materials' widespread biomedical applications[107].

3.3 Strategies for enhancing thermoelectric antimicrobial therapy

Bacterial infections, exacerbated by widespread misuse of antibiotics and multidrug resistance, pose an increasingly serious threat to individual and public health, and cases of failure of conventional antibiotic therapy are commonplace[108]. In this context, the development of antimicrobial drugs with both efficacy and biocompatibility has become an urgent need to deal with drug-resistant bacteria[109,110]. With the exploration of new strategies for infection control, the anti-infective effect of TE materials has been well demonstrated through a series of in vitro antimicrobial tests and in vivo anti-infection modeling studies. Here, we discuss ways to enhance the anti-infective ability of TE materials based on their therapeutic examples.

An effective and simple TE catalytic therapeutic strategy is the controlled release design of antimicrobials. By doping the TE materials with antimicrobial substances, the TE materials are

endowed with active bacterial inhibition to solve the problem of traumatic infection while maintaining their TE properties. For example, Gao et al.[16] doped the constructed TE hydrogel with tannic acid (TA) with antibacterial and anti-inflammatory properties in Figure 7E, which has the ability to disrupt the integrity of bacterial cell membranes and interfere with bacterial energy metabolism, thus inhibiting bacterial growth. In Figure 7A–C, the antibacterial properties against methicillin-resistant *Staphylococcus aureus* (MRSA) and *Escherichia coli* were significantly enhanced with the increase of TA content in the hydrogel. This is because TA can interact with proteins and lipids on the bacterial cell membrane, disrupting the structure and function of the cell membrane and leading to leakage of bacterial contents, as well as interfering with the bacterial energy-producing process so that the bacteria are unable to grow and multiply normally. Meanwhile, excessive ROS at the wound will hinder wound healing. Figure 7D demonstrated that TA has a strong antioxidant capacity, which can effectively scavenge excessive ROS, reduce ROS-induced lipid peroxidation and DNA damage, and protect the tissues and cells from oxidative stress. TA is released into the wound environment, which can react with ROS and convert them into harmless substances, reduce the damage of oxidative stress on tissues and cells, and promote wound healing[16]. Furthermore, Alipuly et al.[111] constructed a hydrogel system of PANI using phytic acid and tested for antimicrobial activity. Since phytic acid is a multivalent acid, it contains several phosphate groups. These phosphate groups can interact with metal ions and proteins on the surface of bacterial cells and interfere with the normal physiological metabolic processes of bacteria. The phosphate group can bind with metal ions on the bacterial cell membrane, destroying the integrity of the cell membrane and leading to the leakage of intracellular substances, thus inhibiting bacterial growth and reproduction; it may also interfere with enzyme activities in the body of the bacteria, affecting processes such as energy metabolism and substance synthesis of the bacteria, and thus exerting an antimicrobial effect. Therefore, as shown in Figure 7F, the hydrogel containing phytic acid showed a certain inhibitory effect on both Gram-positive bacteria (*S. aureus* ATTC12600) and Gram-negative bacteria (*E. coli* ATTC25922)[111].

Inflammatory reaction at the wound slows down the healing process[113], and multimodal treatment with TE materials can effectively modulate inflammation. Electrical stimulation has been demonstrated to suppress bacterial proliferation by perturbing bacterial cell membrane potential and disrupting intracellular metabolic pathways[114]. An illustrative example of this strategy is found in the work of Barman, whose design features a synergistic inhibition of bacterial growth and promotion of wound healing based on both thermal catalysis and electrical stimulation, consisting of TE-catalyzed analytical Bi_2Te_3 nanoplates (Bi_2Te_3 nanoparticles) acting on carbon fiber fabric electrodes. Figure 7G demonstrates that the Bi_2Te_3 material nanoplates (Bi_2Te_3NPs) have excellent ROS generation capability. The generated H_2O_2 has an antibacterial effect and is capable of destroying the cell membrane and intracellular biomolecules of bacteria, thus effectively inhibiting the growth of bacteria against *E.coli* and *S. aureus*. By connecting the integrated electrodes to a wearable friction nanogenerator (triboelectric nanogenerator [TENG]), the internal friction electric layer contacts and separates when subjected to external mechanical forces, resulting in charge transfer and the generation of electrical energy. The electrical stimulation generated by the TENG activates growth factors that promote cell proliferation, migration, and angiogenesis[112]. This hybrid treatment not only acts as an antimicrobial agent but also accelerates wound healing. In addition, photothermolysis has a significant inhibitory and killing effect on bacteria, showing great potential in the antimicrobial field, while, as an effective antimicrobial treatment, the use of the near-infrared (NIR) region[115]. Wang et al.[70], focusing on bacterial infection wound treatment, reduced graphene oxide modified Bi_2Te_3 nanosheets (rGO-Bi_2Te_3) based on reduced graphene oxide were developed, which were experimentally demonstrated to be highly effective antibacterial against both *S. aureus* and *MRSA* in vitro and in vivo. The rGO-Bi_2Te_3 nanosheets were integrated into polyurethane fibers to make an electrostatically spun film, and the antimicrobial therapy was achieved by using near-infrared light irradiation. Figure 7H demonstrated a photothermal electrocatalytic mechanism based on the fact that under NIR light irradiation, the Bi_2Te_3 excitation produces photogenerated electrons and hot carriers, and the electrons migrate from the Bi_2Te_3 to the rGO, which efficiently separates the electron-cavity pairs to produce a large number of ROS with strong oxidizing property can destroy the bacterial cell membrane and internal proteins to inhibit bacterial growth. At the same time, the good photothermal performance of rGO-Bi_2Te_3 increases the temperature, and the thermal effect synergizes with ROS to accelerate bacterial death. In addition, rGO provides additional carrier transport channels to enhance the TE properties and promote charge transfer and separation, further enhancing the antibacterial effect[70]. Combination with other substances or materials can activate or amplify the therapeutic effect, and combined with biocompatibility assessment, suggests that TE materials hold significant promise for antimicrobial therapy.

4. Strategies for enhancing property of thermoelectric materials

TE materials enable the direct interconversion of thermal and electrical energy. The *S* directly affects the intensity of electrical stimulation and the enhancement effect of endogenous EF by determining the temperature difference-to-electrical energy conversion efficiency. A high Seebeck coefficient can generate sufficient electrical stimulation under physiological temperature differences; this stimulation regulates cellular behavior and angiogenic signaling pathways, ultimately accelerating the wound-healing process[55]. Optimizing their TE properties improves the efficiency of this conversion, enabling better use of the thermal portion of renewable energy sources without any moving parts or emissions, and creating localized cooling for the thermal management of advanced electronic devices and human comfort[116]. TE properties are usually measured by the TE ZT, where the higher the ZT, the better the performance of the material. To increase the ZT, various strategies focus on optimizing the thermal transport properties by reducing the lattice thermal conductivity[117] and optimizing electron transport properties by manipulating carrier concentration, mobility, and energy band engineering[118]. While breakthroughs have been made in the former, progress in the latter has not been as rapid. As the thermal conductivity of TE materials approaches the minimum theoretical limit, it is necessary to make a shift toward increasing the TE PF in the process of increasing the ZT[119].

4.1 Electrical transmission performance optimization

The TE property enhancement of TE materials is mainly achieved by optimizing the ZT, which requires the synergistic regulation of the electrical transport properties (Seebeck coefficient S, electrical conductivity σ) and thermal transport properties (thermal conductivity κ). The core objective of the electrical transport properties optimization is to enhance the PF of the material, to increase the *S* and σ at the same time. Since there is a natural trade-off between *S* and σ, where high carrier concentration decreases *S* and vice versa, this limitation needs to be addressed by the following strategy:

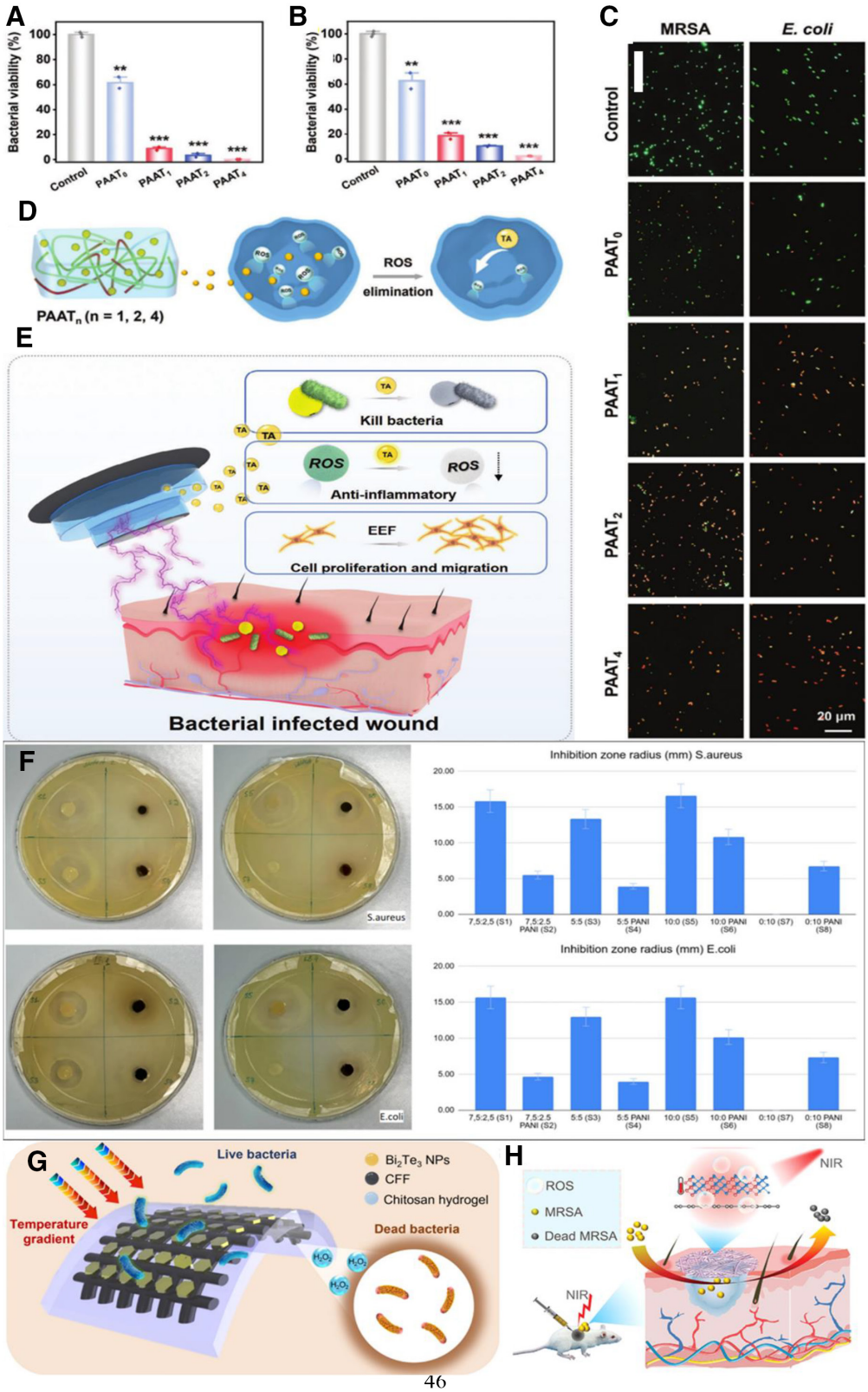

46

Figure 7. Antibacterial properties of thermoelectric dressings. (A) MRSA and (B) E. coli after treatment with the synthesized hydrogels. The error bars are based on the SDs ($n = 3$). Note: $^{*}P < 0.05$, $^{**}P < 0.01$, and $^{***}P < 0.001$. (C) Live/dead fluorescence staining images of MRSA and E. coli after different treatments (scale bar: 20 μm). (D) Schematic diagram of the release of TA from the hydrogels to eliminate intracellular ROS. (E) Schematic diagram illustrating under the natural temperature difference between infected wounds and the external environment and can exert bactericidal, anti-inflammatory, and cell migration effects by releasing TA and reshaping the EEF, promoting wound healing[16]. Copyright 2024, Wiley-VCH GmbH. (F) Antibacterial test results based on growth inhibition zones of S.aureus and E.coli. S1 and S2 (7.5:2.5 without and with PANI); S3 and S4 (5:5 without and with PANI); S5 and S6 (10:0 without and with PANI); S7 and S8 (0:10 without and with PANI) respectively[111]. Copyright 2024, The Mukhtar Alipulys. (G) Schematic representation of the antibacterial mechanism of Bi_2Te_3 NPs[112]. Copyright 2023, The Snigdha Roy Barmans. (H) Mechanism of rGO-Bi_2Te_3 therapy for MRSA wound infections in vivo[70]. Copyright 2022, Wiley-VCH GmbH. MRSA, methicillin-resistant Staphylococcus aureus; PANI, polyaniline; rGO-Bi_2Te_3, reduced graphene oxide modified Bi_2Te_3; ROS, reactive oxygen species; TA, tannic acid.

4.1.1 Carrier concentration optimization

Optimization of the TE ZT can be achieved through meticulous control of the doping level. Such high-efficiency doping strategies enable precise engineering of carrier concentration, thereby allowing for fine-tuned manipulation of the Fermi level during material synthesis[120]. Therefore, the carrier concentration can be regulated by doping to be at or near the optimal concentration[121]. Doping has been widely used to activate additional electrons (n-type doping) or holes (p-type doping) to regulate the carrier concentration of a subject[122]. Cheng et al.[123] TE properties of β-$FeSi_2$ were optimized with phosphorus (P) doping at 850 K, $FeSi_{1.96}P_{0.04}$has the highest TE optimum ZT of about 0.12, which is much higher than the results of previous studies (the highest ZT is only 0.03 at 673 K). Meanwhile, the carrier concentration of P-doped β-$FeSi_2$ was changed, the highest was about10^{20} cm^{-3}[123]. Meanwhile, Hou et al.[124] investigated the effects of indium (In) doping and copper (Cu) dynamic doping on the TE properties of n-type PbS. It acted as a donor atom, replacing the Pb site to introduce free electrons into PbS, and when the indium doping concentration x = 0.0015, in Figure 8A, the carrier concentration was enhanced from 1.7×10^{16} to 3×10^{20}/cm^3, which synergistically improves the conductivity and Seebeck coefficient, resulting in a room temperature PF of 12.3 μW/cm/K^2 for the PbS sample with a ZT value of 0.7. After that, Cu atoms are introduced to realize the dynamic doping, which optimizes the carrier concentration in the high-temperature region and enlarges the effective mass of the carriers, and further improves the PF in a wide temperature domain. Figure 8B shows the $Pb_{0.995}In_{0.005}S$ + 3% Cu sample, the PF reaches a peak of 21.7 μW/cm/K^2 at 573 K, and the average PF reaches 18.8 μW/cm/K^2 at 423–823 K, and the average ZT value is improved from 0.4 to 0.8[124]. Carrier concentration optimization has significant advantages in enhancing TE properties, but it also has certain limitations. It faces problems such as low solubility of dopant elements, difficulty in precise control, and mutual constraints of each parameter in practical applications, which are yet to be further investigated.

4.1.2 Energy band engineering

Because energy band features are intrinsic to certain crystals, it is possible to optimize the carrier effective mass (m^*) and density of states (DOSs) by modulating the energy band structure of the material, thereby enhancing the PF[42]. "Carrier pocket engineering" has been demonstrated as an effective means of increasing m^*[127]. It is shown that the temperature-dependent shifts of the 2 valence bands of the $PbTe_{1-x}Se_x$ alloy at L (degeneracy = 4) and Σ (degeneracy = 12) lead to their energy convergence in the mid-temperature region and separation at high temperatures[128]. Pei et al.[129] regulated the energy band structure engineering modulation of PbTe through Se and Sr alloying, as shown in Figure 8C, resulted in an enhancement of the ZT value of the material at 300 to 923 K. The energy band structure of PbTe was modified by Se alloying. In the $PbTe_{1-x}Se_x$-2Na-4SrTe system, Se alloying diverges the L and Σ valence bands, altering the energy band structure and pushing the PF maximum to higher temperatures, as well as decreasing the energy shift between the L and Σ valence bands and increasing the Seebeck coefficients. The $PbTe_{1-x}Se_x$-2Na-4SrTe reaches a ZT of 2.3 at 923 K, and the average ZT from 300 to 873 K is 1.23, which corresponds to an increase in PF and TE conversion efficiency[129]. Since the electron DOS and its energy dependence around the Fermi energy level dominate electron transport, proper engineering of the DOS is also expected to achieve high PF. Particular interest is electronic band distortions involving the so-called resonance energy levels[125]. Zhao et al.[130] found that after filling $CoSb_3$ with indium (In), the 5p orbital hybridization of In with Sb enhances the p-d orbital hybridization of Co with Sb, resulting in a change in the energy band structure near the Fermi energy level. This is specifically manifested as the Fermi energy level enters the conduction band, the DOS at the bottom of the conduction band increases significantly, and the DOS at the top of the valence band decreases, and this asymmetric distribution is conducive to obtaining high Seebeck coefficients and conductivities[130].

4.1.3 Enhanced carrier mobility

Although band degeneracy[128,131,132]and DOSs[133,134] have been widely employed to tune the Fermi level and band characteristics, they also scatter charge carriers and exert adverse effects on carrier mobility (μ)[135,136]. To further enhance the wide temperature range performance of TE materials, it is necessary to optimize other electrical parameters and reduce the thermal conductivity of the system while maintaining a high carrier mobility[137].

$$\sigma = ne\mu, \tag{4}$$

In addition, μ is a key parameter to determine the electrical conductivity of TE materials, and thus, the enhancement of carrier mobility can enable the system to obtain high electrical transport performance and PF in a wide temperature range. On the one hand, a substantial increase in carrier mobility can be realized by crystal defect modulation[117]. By rationally tuning the defect types and densities, a substantial increase in carrier mobility can be realized. In their study on the TE material BiCuSeO, Li et al.[117] altered the material's microstructure and electronic properties through Na doping, thereby influencing its carrier mobility and electrical conductivity. Compared with doping by other alkaline earth metals (such as Sr, Ba, and Mg), Na-doped samples exhibit higher carrier mobility (μ = 8 cm^2/V/s) at the same carrier concentration. This is because the ionic radius difference between Na^+ and Bi^{3+} is relatively small (approximately 0.01 Å), leading to weaker point defect scattering of charge carriers. As a result, Na doping can increase the carrier concentration while causing relatively minor damage to mobility. Specifically, Na doping not only enhances the carrier concentration and improves the electrical conductivity but also, although the Seebeck coefficient decreases slightly with the increase in Na doping amount, the decrease amplitude is relatively small. Moreover, by reducing the lattice thermal conductivity, a significant improvement in the ZT value is ultimately achieved[138]. On the other hand, modulation doping (MD) has been demonstrated to successfully address the mobility degradation caused by alloying and enhance carrier mobility[126,139,140]. MD has been widely used in 2-dimensional electron gas thin-film devices to improve carrier mobility[141], thereby enhancing electrical conductivity. This strategy has also been successfully applied in the TE field to optimize the electrical properties of SiGe-based bulk composite TE materials[138,139]. Figure 8D illustrates that MD enhances carrier mobility by separating charge carriers from ionized impurities to reduce charge scattering. In this approach, dopants are introduced only into 1 type of nanoparticle, and charge carriers spill over from the doped nanoparticles into the undoped or lightly doped matrix phase, increasing the spatial distance between ionized nanoparticles. In conventional uniform heavy doping, ionized impurities strongly scatter charges, whereas MD reduces such scattering, thereby improving carrier mobility. Taking SiGe alloy nanocomposites as an example, by selecting appropriate nanoparticles (e.g., $Si_{70}Ge_{30}P_3$) and a matrix ($Si_{95}Ge_5$), type-II band alignment is formed between them (Figure 8E), where the conduction band edge of the nanoparticles is relatively higher, promoting carrier flow into the matrix. Meanwhile, the matrix with a higher Si content has a larger effective mass of the DOSs, providing more fillable energy states for carriers, which is favorable for carrier migration and further improves carrier mobility[140]. Therefore, in material systems with low carrier mobility, MD is a feasible method to enhance carrier mobility and optimize TE performance.

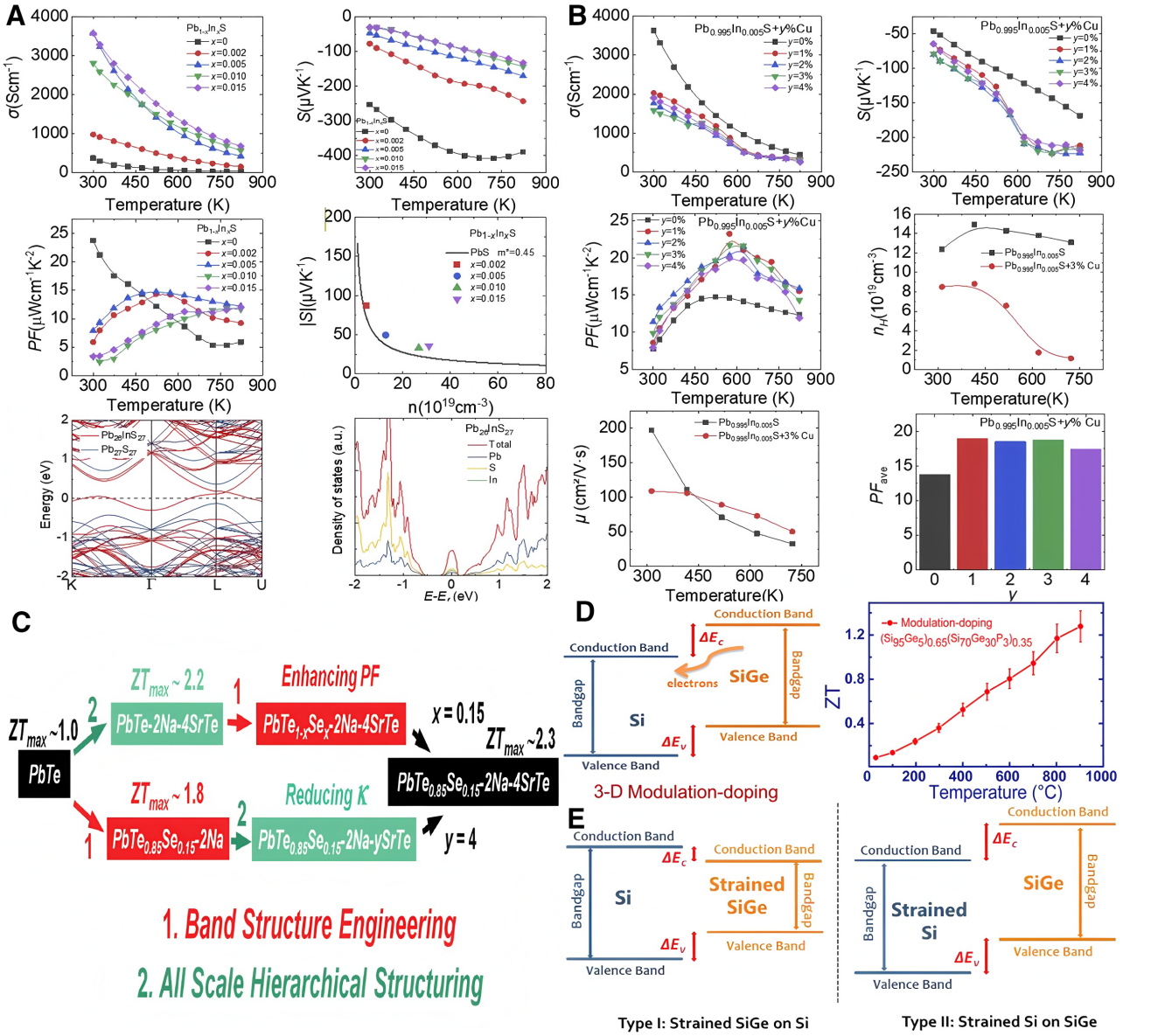

Figure 8. Methods for enhancing the performance of thermoelectric materials. (A) Temperature dependence of thermoelectric performance of $Pb_{1-x}In_xS$ (x = 0, 0.002, 0.005, 0.010, 0.015) samples. (B) Temperature dependence of electrical transport properties of $Pb_{0.995}In_{0.005}S$ + y% Cu (y = 0, 1, 2, 3, 4)[42]. Copyright 2021, Elsevier. (C) Alternate roadmaps toward high thermoelectric performance achieved in PbTe0.85Se0.15-2Na-4SrTe sample via integration of band structure engineering with all-scale hierarchical structuring[125]. Copyright 2016, Wiley-VCH GmbH. (D) Modulation-doping was theoretically proposed and experimentally proved to be effective in increasing the power factor of nanocomposites $(Si_{80}Ge_{20})_{70}(Si_{100}B_5)_{30}$ by increasing the carrier mobility but not the ZT due to the increased thermal conductivity. (E) Type I (strained SiGe on Si) and type-II (strained Si on SiGe) band alignments[126]. Copyright 2012, American Chemical Society.

4.2 Thermal conductivity reduction strategies

The central aim of optimizing thermal transport properties is to reduce the thermal conductivity (κ) of materials, which consists of 2 components: electronic thermal conductivity (κ_e) and lattice thermal conductivity (κ_l). Electronic thermal conductivity adheres to the Wiedemann-Franz law,

$$\kappa_e = L\sigma T, \tag{5}$$

where L represents the Lorenz number. Evidently, κ_e exhibits a direct proportionality to electrical conductivity (σ). In contrast, lattice thermal conductivity can be tuned relatively independently, rendering its reduction an effective strategy for enhancing thermal transport performance[142–146]. Since lattice thermal conductivity is governed by phonon propagation, suppressing heat conduction through enhanced phonon scattering becomes crucial. High-symmetry cubic structured materials (e.g., PbTe, SnTe) require special properties such as phonon nesting and avoiding crossing to induce strong anharmonicity, thereby reducing κ_l. Low-symmetry structured materials (e.g., SnSe and Ag_8SnSe_6) can enhance phonon scattering via multiple mechanisms, including lone-pair electrons, weak interlayer interactions, vacancies, and ion diffusion, inherently possessing low κ_l. Defect engineering (e.g., doping and vacancy introduction) and nanostructure self-assembly (e.g., the superlattice of $AgSbTe_2$) are effective approaches to regulating phonon properties[147]. When the grain size of $CoSb_3$ is reduced from the microscale to the nanoscale, both lattice thermal conductivity and the overall thermal conductivity of the TE material decrease significantly. Specifically, reducing the grain size from 1 μm to 100 nm lowers the thermal conductivity at room temperature from 10.67 to 3.84 W/m/K, and further decreasing it to 50 nm

reduces the conductivity to 1.44 W/m/K. This trend underscores that a lower lattice thermal conductivity is advantageous for improving TE performance. The underlying mechanism lies in the nanostructuring of the $CoSb_3$ compound: as the grain size diminishes, the mean free path (d_1) of phonons shortens. Concurrently, the increased surface-to-volume ratio of the material amplifies phonon scattering at interfaces, thereby reducing both d_1 and the average phonon velocity (ν_1). According to the formula for lattice thermal conductivity,

$$\kappa_1 = 1/3\ C_v v_1 d_1, \quad (6)$$

these reductions in d_1 and ν_1 lead to a substantial decline in κ_1[148].

Topological insulators (TIs) are quantum materials with unique electronic structures, featuring insulating bulk states and topologically protected conducting states on their surfaces or edges. Studies have shown that TIs can exhibit extremely low lattice thermal conductivity[144,149,150], and their distinctive surface conductivity holds promise to break through the limitations of semiconductor-based TE materials, achieving dual optimization of electrical and thermal properties. TIs inherently possess low κ_1 due to strong spin-orbit coupling induced by heavy atoms. Additionally, their unique band inversion drives the generation of non-parabolic warping in conduction bands/valence bands, and this warping effect can enhance weighted mobility by reducing the electrical conductivity effective mass and increasing the Seebeck effective mass[151]. These 2 effects synergistically optimize the balance among electrical conductivity, Seebeck coefficient, and thermal conductivity. The influence of their surface states on TE performance is regulated by the surface-to-volume ratio, temperature (with a significant effect at temperatures below 200 K), and Fermi level: the higher the surface-to-volume ratio, the greater the contribution of surface states; as temperature increases, bulk states become dominant; and the Fermi level regulates the contribution ratio between surface and bulk states. The offsetting effect of surface states can be weakened through targeted regulation. The core strategies for enhancing their bulk TE performance include 3 categories: Mechanical strain and external pressure enhance the strength of band inversion by strengthening atomic orbital interactions[152], alloying regulates lattice parameters and orbital interactions through chemical pressure or elemental substitution[151], topological phase transitions optimize carrier transport near the critical composition by forming alloys of conventional insulators and TIs[153]. All 3 strategies achieve performance enhancement by focusing on strengthening band inversion and optimizing band structure[154].

However, a single regulatory approach is often difficult to break through the performance bottleneck. Ma's group adopted a multidimensional synergistic strategy encompassing "single crystal growth, composition regulation, crystal structure and band engineering, and bipolar conduction suppression," simultaneously achieving the enhancement of electrical transport efficiency and precise inhibition of thermal conduction[155]. First, Mg_3Bi_2-based single crystals were precisely synthesized via a slow cooling method, which effectively eliminates grain boundaries and various defects commonly present in polycrystalline materials, reduces scattering losses during carrier transport, significantly enhances carrier mobility, and thereby lowers the electrical resistivity of the material, laying a solid foundation for optimizing electrical transport performance[156,157]. Second, through a composition regulation scheme involving Sb substitution for Bi[158], trace Te doping, and Mg excess design, the carrier concentration was accurately fine-tuned to the optimal range while optimizing carrier transport characteristics. This avoids a significant drop in the Seebeck coefficient under the premise of ensuring high electrical conductivity, realizing an efficient improvement in the PF. Third, leveraging the unique anti-La_2O_3-type layered structure and 3D atomic bonding network of Mg_3Bi_2-based single crystals, near-isotropic charge transport channels were constructed. The electrical conductivity effective mass exhibits minimal difference between the ab-plane ($0.24m_0$) and c-plane ($0.21m_0$), which not only guarantees carrier transport efficiency in all directions but also enhances phonon scattering through structural distortion and atomic size differences. This effectively reduces the lattice thermal conductivity (κ_1), achieving a dynamic balance between electrical transport and thermal conduction[159,160]. Fourth, the bipolar conduction effect was suppressed by optimizing the band structure, avoiding the attenuation of the Seebeck coefficient and increase in thermal conductivity caused by the simultaneous participation of electrons and holes in transport—addressing the critical issue of performance degradation in traditional $Bi_2(Te, Se)_3$ materials at elevated temperatures[161]. Under the synergistic effect of the multidimensional strategy, the $Mg_3Bi_{1.497}Sb_{0.5}Te_{0.003}$ single crystal ultimately achieved a ZT value of 1.05 at 300 K and 0.87 at 250 K[162], which is significantly superior to commercial n-type $Bi_2(Te, Se)_3$ materials. Moreover, it maintains high performance above 350 K, successfully expanding the temperature application range for high ZT values. This fully confirms the core logic that the improvement of TE performance requires the synergistic efforts of multiple approaches.

5. Challenges and future prospects

5.1 Challenges in thermoelectric materials for wound healing

Despite the promising potential, the clinical translation of TE materials for wound healing faces several formidable challenges. First, a significant hurdle lies in the biosafety-performance paradox. Most inorganic TE materials with high ZT values (e.g., Bi_2Te_3) raise biosafety concerns due to the potential leaching of toxic ions (e.g., Te^{4-}) upon long-term implantation, necessitating complex encapsulation strategies[56]that may compromise flexibility and performance. Conversely, organic TE materials (e.g., PEDOT:PSS, PANI) offer superior biocompatibility and flexibility but generally exhibit inferior TE properties (lower σ and S)[38] that require substantial optimization to generate therapeutic electrical signals efficiently.

Another challenge in the use of TE materials in wound therapy is optimizing the TE properties of TE materials at room temperature. The optimal TE properties of some TE materials act at higher temperatures than room temperature[163]. More precise strategies, such as elemental doping, surface modification, and interfacial engineering, are needed to address this problem. In addition, wound dressing matrices require innovative design in materials and devices to provide safe, stable, and effective TE therapy and to maximize the temperature gradient in wound care.

Beyond the aforementioned issues, there is currently no unified good manufacturing practice (GMP) standard for TE hydrogels/devices, thus hindering the acquisition of regulatory approval[164]. Furthermore, divergent classification criteria for TE hydrogels/devices across different countries/regions, coupled with variations in GMP requirements for TE materials, further exacerbate certification complexity.

5.2 Prospects in thermoelectric materials for wound healing

In recent years, many research works have focused on TE materials, and the results have fully demonstrated the promising development of these materials in the field of wound healing. As research continues, the development of TE materials with excellent antimicrobial efficacy, biocompatibility, intelligence, and multifunctional properties has become a promising research direction. Based on this, we systematically analyze and propose several cutting-edge strategies for the design and preparation of

TE materials, aiming to provide more efficient, safer, and more precise therapeutic solutions for wound healing, with a view to promoting technological innovation and clinical translation in this field.

(1) Multimodal synergistic therapy: Combining TE material-based antimicrobial drug therapy with other mechanisms to promote wound healing[165]. Through the design of composite functions, a combination of drug sustained-release systems, antibacterial coatings, piezoelectric materials, and photocatalytic materials is integrated to develop multifunctional devices, such as smart temperature sensors, thermal sensors, TE modules, and trigger circuits[166]. These multifunctional devices can realize synergistic therapy in applications such as low-grade thermal energy harvesting, temperature sensing, and self-powered electronic devices, thereby enhancing the therapeutic effect. Furthermore, we can draw on the ideas of synergistic design between energy storage facilities and energy systems, as well as multi-energy complementarity, to enhance energy supply stability[167], thereby achieving a long-term stable energy supply for chronic wounds.
(2) Material design: The development of Te-free inorganic materials (e.g., Ag_2Se) and the hybridization of high-performance inorganic fillers within biocompatible organic matrices (e.g., hydrogels, polymers) represent a promising path to break the biosafety-performance trade-off. Concurrently, advancing the molecular design of organic semiconductors and nanostructuring techniques is crucial to enhance the electrical conductivity and Seebeck coefficient of flexible organic TE materials[168]. In addition, to avoid insufficient temperature difference resulting from excessively high ambient temperature, diurnal cooling technology can be integrated with the cold side of the TE wound dressing to maintain an optimal temperature difference[169].
(3) Advancing clinical translation and standardization: Bridging the gap between laboratory research and clinical practice is paramount. This requires establishing standardized protocols for evaluating the long-term biosafety, stability, and efficacy of TE devices in biologically relevant environments. Large-scale animal studies and eventual pilot clinical trials on various wound types (e.g., diabetic ulcers[170,171], burns) are essential to validate therapeutic outcomes. Moreover, efforts should be directed toward scalable manufacturing processes (e.g., 3D printing, roll-to-roll processing) and cost reduction to facilitate future commercialization and widespread accessibility[172].
(4) Cooperation between universities and GMP-certified enterprises should be pursued to develop specialized guidelines for TE materials as medical devices, clarify product classification and testing standards, and shorten the approval cycle. Meanwhile, TE raw material suppliers should collaborate with GMP-certified chemical enterprises to establish a standardized raw material production system. Additionally, equipment manufacturers are encouraged to partner with medical device companies to modify specialized equipment to meet GMP requirements.

These innovations will not only promote the upgrading of treatment modalities but also help expand clinical applications. Through standardization and cost optimization, TE materials will play a greater role in chronic wound repair and postoperative rehabilitation, fundamentally revolutionizing the concept and practice of wound treatment and bringing patients a more efficient and better treatment experience.

6. Conclusion

The integration of TE materials into the field of skin therapeutics has transformative potential and promises to raise the standard of care for skin regeneration and repair. As evidenced by the numerous research and innovation advances in this field, the convergence of biomedical engineering, materials science, and nanotechnology can propel us to unprecedented advances in healthcare. Possessing the unique property of utilizing temperature differences to generate electrical currents makes TE materials ideal for treating skin wounds. This electrical activity is critical in regulating cellular functions such as proliferation, differentiation, and matrix production, all of which are key to skin cell regeneration. This article reviews the TE effect, mechanisms of electrical stimulation of skin cells, classification of TE materials, and various applications. To further advance the use of TE materials in anti-infective therapies, we discuss the principles of TE material design in the biomedical field, encompassing good mechanical properties as well as excellent biocompatibility. We further discuss methodological strategies to optimize electrical transport properties and reduce thermal conductivity to improve TE properties. Finally, we summarize the issues facing the future development of TE materials in the field of therapeutic skin, as well as future prospects. The promotion of cell migration and angiogenesis by TE materials can significantly shorten the healing time and improve patient outcomes, providing new ideas for the treatment of skin wound healing in the medical field.

Acknowledgements

This work was financially supported by the National Natural Science Foundation of China (Grant No. 32571629), the Natural Science Foundation of Liaoning Province (Grant Nos. 2024011874-JH4/4800 and 2023011989-JH3/4600), the Scientific Research Projects of Liaoning Provincial Department of Education (Grant No. LJ212410163004), and the Career Development Support Program for Young and Middle-aged Teachers of Shenyang Pharmaceutical University (Grant No. ZQN202208).

Conflicts of interest

The authors declare that they have no conflicts of interest.

Data availability statement

No primary research results, software, or code have been included, and no new data were generated or analyzed as part of this review.

Author contributions

Ying Zhang: Writing–original draft, investigation, visualization; Zhining Hao: Formal analysis, visualization; Zhou Li: Methodology, resources; Yiping Mu: Conceptualization, funding acquisition; Zhaoxu Meng: Project administration, writing–review & editing, funding acquisition; He Lian: Writing–original draft, writing–review & editing, funding acquisition, supervision.

References

[1] Hsu CK, Lin HH, Harn HI, et al. Mechanical forces in skin disorders. *J Dermatol Sci*. 2018;90:232–240.
[2] Dąbrowska AK, Spano F, Derler S, et al. The relationship between skin function, barrier properties, and body-dependent factors. *Skin Res Technol*. 2018;24:165–174.
[3] Gould J. Superpowered skin. *Nature*. 2018;563:S84–S85.
[4] Liu M, Chen Y, Zhu Q, et al. Antioxidant thermogelling formulation for burn wound healing. *Chem Asian J*. 2022;17:e202200396.
[5] Roberts CD, Leaper DJ, Assadian O. The role of topical antiseptic agents within antimicrobial stewardship strategies for prevention and treatment of surgical site and chronic open wound infection. *Adv Wound Care*. 2017;6:63–71.

[6] Sen CK. Human wound and its burden: updated 2025 compendium of estimates. *Adv Wound Care*. 2025;14:429–438.
[7] Kwon JH, Powderly WG. The post-antibiotic era is here. *Science*. 2021;373:471.
[8] Pereira RF, Bártolo PJ. Traditional therapies for skin wound healing. *Adv Wound Care*. 2016;5:208–229.
[9] Tören E, Mazari AA. Pullulan/collagen scaffolds promote chronic wound healing via mesenchymal stem cells. *Micro*. 2024;4:599–620.
[10] Yu B, Li Z, Huang S. The application of ultrasound for skin and appendage regeneration: a comprehensive review. *Innovation Life*. 2024;2:100074.
[11] Shi XL, Zou J, Chen ZG. Advanced thermoelectric design: from materials and structures to devices. *Chem Rev*. 2020;120:7399–7515.
[12] Lee H. The Thomson effect and the ideal equation on thermoelectric coolers. *Energy*. 2013;56:61–69.
[13] Zhang M, Tian Y, Xie H, et al. Influence of Thomson effect on the thermoelectric generator. *Int J Heat Mass Transfer*. 2019;137:1183–1190.
[14] Yang H, Lin C, Liang K, et al. High-performance double-stage Mg_3Bi_2-based thermoelectric cooler. *Innov Mater*. 2025;3:100130.
[15] Snyder GJ, Toberer ES. Complex thermoelectric materials. *Nat Mater*. 2008;7:105–114.
[16] Gao S, Rao Y, Wang X, et al. Skin temperature-activated multifunctional thermoelectric dressing for bacterial infected wound treatment. *Adv Funct Mater*. 2024;35:2415085.
[17] Sattar M, Yeo WH. Recent advances in materials for wearable thermoelectric generators and biosensing devices. *Materials (Basel, Switzerland)*. 2022;15:4315.
[18] Snyder GJ, Snyder AH. Figure of merit ZT of a thermoelectric device defined from materials properties. *Energy Environ Sci*. 2017;10:2280–2283.
[19] Ma Z, Wei J, Song P, et al. Review of experimental approaches for improving zT of thermoelectric materials. *Mater Sci Semicond Process*. 2021;121:105303.
[20] Meng B, Liu J, Wang L. Recent development of n-type thermoelectric materials based on conjugated polymers. *Nano Mat Sci*. 2021;3:113–123.
[21] Lu Y, Wang JY, Pei J. Strategies to enhance the conductivity of n-type polymer thermoelectric materials. *Chem Mater*. 2019;31:6412–6423.
[22] Singh NK, Bathula S, Gahtori B, et al. The effect of doping on thermoelectric performance of p-type SnSe: promising thermoelectric material. *J Alloys Compd*. 2016;668:152–158.
[23] Xu L, Liu Y, Chen B, et al. Enhancement in thermoelectric properties using a P-type and N-type thin-film device structure. *Polym Compos*. 2013;34:1728–1734.
[24] Gao M, Luo Y, Li W, et al. In vitro and in vivo biocompatibility assessment of chalcogenide thermoelectrics as implants. *J Mater Chem B*. 2024;12:6847–6855.
[25] Kong D, Zhu W, Guo Z, et al. High-performance flexible Bi_2Te_3 films based wearable thermoelectric generator for energy harvesting. *Energy*. 2019;175:292–299.
[26] Ding Y, Qiu Y, Cai K, et al. High performance n-type Ag_2Se film on nylon membrane for flexible thermoelectric power generator. *Nat Commun*. 2019;10:841.
[27] Zhang S, Fan Z, Wang X, et al. Enhancement of the thermoelectric properties of PEDOT:PSS via one-step treatment with cosolvents or their solutions of organic salts. *J Mater Chem A*. 2018;6:7080–7087.
[28] Seiti M, Giuri A, Corcione CE, et al. Advancements in tailoring PEDOT: PSS properties for bioelectronic applications: a comprehensive review. *Biomater Adv*. 2023;154:213655.
[29] Shalini V, Navaneethan M, Harish S, et al. Design and fabrication of PANI/GO system for enhanced room-temperature thermoelectric application. *Appl Surf Sci*. 2019;493:1350–1360.
[30] Goo G, Anoop G, Unithrattil S, et al. Proton-irradiation effects on the thermoelectric properties of flexible Bi_2Te_3/PEDOT: PSS composite films. *Adv Electron Mater*. 2019;5:1800786.
[31] Lim JY, Cho S, Kim H, et al. Optimum thermoelectric performance of bismuth–antimony–telluride alloy/PEDOT: PSS nanocomposites prepared by an innovative redox process. *ACS Appl Energy Mater*. 2019;2:8219–8228.
[32] Jia Y, Jiang Q, Sun H, et al. Wearable thermoelectric materials and devices for self-powered electronic systems. *Adv Mater*. 2021;33:2102990.
[33] Jiang S, Li H, Zhang L, et al. Generic Diagramming Platform (GDP): a comprehensive database of high-quality biomedical graphics. *Nucleic Acids Res*. 2025;53:D1670–D1676.
[34] Chen WY, Shi XL, Zou J, et al. Thermoelectric coolers: progress, challenges, and opportunities. *Small Met*. 2022;6:2101235.
[35] Dughaish ZH. Lead telluride as a thermoelectric material for thermoelectric power generation. *Physica B*. 2002;322:205–223.
[36] Liu ZY, Zhu JL, Tong X, et al. A review of $CoSb_3$-based skutterudite thermoelectric materials. *J Adv Ceram*. 2020;843:156063.
[37] Chen S, Ren Z. Recent progress of half-Heusler for moderate temperature thermoelectric applications. *Mater Today*. 2013;16:387–395.
[38] Russ B, Glaudell A, Urban JJ, et al. Organic thermoelectric materials for energy harvesting and temperature control. *Nat Rev Mater*. 2016;1:16050.
[39] Xu SD, Hong M, Shi XL, et al. High-performance PEDOT: PSS flexible thermoelectric materials and their devices by triple post-treatments. *Chem Mater*. 2019;31:5238–5244.
[40] Lo LW, Zhao J, Wan H, et al. An inkjet-printed PEDOT: PSS-based stretchable conductor for wearable health monitoring device applications. *ACS Appl Mater Interfaces*. 2021;13:21693–21702.
[41] Jun L, Zhang LM, Li H, et al. Synthesis and thermoelectric properties of polyaniline. *J Wuhan Uni Tech-Mater Sci Ed*. 2003;18:53–55.
[42] Han H, Zhao L, Wu X, et al. Advancements in thermoelectric materials: optimization strategies for enhancing energy conversion. *J Mater Chem A*. 2024;12:24041–24083.
[43] Pernstich KP, Rössner B, Batlogg B. Field-effect-modulated Seebeck coefficient in organic semiconductors. *Nat Mater*. 2008;7:321–325.
[44] McCaig CD, Rajnicek AM, Song B, et al. Controlling cell behavior electrically: current views and future potential. *Physiol Rev*. 2005;85:943–978.
[45] Moulin VJ, Dubé J, Rochette-Drouin O, et al. Electric potential across epidermis and its role during wound healing can be studied by using an in vitro reconstructed human skin. *Adv Wound Care*. 2012;1:81–87.
[46] Song JW, Ryu H, Bai W, et al. Bioresorbable, wireless, and battery-free system for electrotherapy and impedance sensing at wound sites. *Sci Adv*. 2023;9:eade4687.
[47] Sun X, Yang YN, Liu Q, et al. Accelerating wound healing with flexible zinc ion microbatteries coupled with endogenous electrical fields. *Nano Energy*. 2024;123:109425.
[48] Cañedo Dorantes L, Caññedo Ayala M. Skin acute wound healing: a comprehensive review. *Int. J. Inflamm*. 2019;2019:3706315.
[49] Greenlee Wacker MC. Clearance of apoptotic neutrophils and resolution of inflammation. *Immunol Rev*. 2016;273:357–370.
[50] Wang N, Liang H, Zen K. Molecular mechanisms that influence the macrophage m1-m2 polarization balance. *Front Immunol*. 2014;5:614.
[51] Chen A, Huang H, Fang S, et al. ROS: A "booster" for chronic inflammation and tumor metastasis. *Biochim Biophys Acta*. 2024;1879:189175.
[52] Akagawa M. Protein carbonylation: molecular mechanisms, biological implications, and analytical approaches. *Free Radical Res*. 2020;55:307–320.
[53] Goswami AG, Basu S, Huda F, et al. An appraisal of vascular endothelial growth factor (VEGF): the dynamic molecule of wound healing and its current clinical applications. *Growth Fact*. 2022;40:73–88.
[54] Zhao D, Tang X, Chen X, et al. Thermoelectric bionic skin promotes diabetic wound healing by restoring bioelectric field microenvironment. *Adv Funct Mater*. 2025;n/a:e22104.
[55] Qin Y, Jia S, Shi XL, et al. Self-powered thermoelectric hydrogels accelerate wound healing. *ACS Nano*. 2025;19:15924–15940.
[56] Zhang Y, Ge B, Feng J, et al. High-performance self-powered flexible thermoelectric device for accelerated wound healing. *Adv Funct Mater*. 2024;34:2403990.
[57] Xin J, Gao L, Zhang W, et al. A thermogalvanic cell dressing for smart wound monitoring and accelerated healing. *Nat Biomed Eng*. 2026;10:80–93.
[58] Lv J, Li X, An Z, et al. A self-powered flexible bioelectronic system based on thermoelectric generator for electrotherapy and monitoring of chronic wounds. *Adv Mater Technol*. 2025;10:e00332.
[59] Sorg H, Tilkorn DJ, Hager S, et al. Skin wound healing: an update on the current knowledge and concepts. *Eur Surg Res*. 2016;58:81–94.
[60] Yazdi MK, Vatanpour V, Taghizadeh A, et al. Hydrogel membranes: a review. *Mater Sci Eng C Mater Biol Appl*. 2020;114:111023.
[61] Liu Z, Liang G, Zhan Y, et al. A soft yet device-level dynamically super-tough supercapacitor enabled by an energy-dissipative dual-crosslinked hydrogel electrolyte. *Nano Energy*. 2019;58:732–742.
[62] Tan M, Liu Y, Wang Y, et al. Wireless thermoelectric hydrogel recreates biomimetic electric field and angiogenic signal accelerating diabetic ulcer repair. *Adv Funct Mater*. 2025;35:2425610.
[63] Zhu T, Ni Y, Biesold GM, et al. Recent advances in conductive hydrogels: classifications, properties, and applications. *Chem Soc Rev*. 2022;52:473–509.

[64] Op 't Veld RC, Walboomers XF, Jansen JA, et al. Design considerations for hydrogel wound dressings: strategic and molecular advances. *Tissue Eng Part B Rev*. 2020;26:230–248.
[65] Mao L, Hu S, Gao Y, et al. Biodegradable and electroactive regenerated bacterial cellulose/MXene ($Ti_3C_2T_x$) composite hydrogel as wound dressing for accelerating skin wound healing under electrical stimulation. *Adv Healthcare Mater*. 2020;9:e2000872.
[66] Zhou T, Yuk H, Hu F, et al. 3D printable high-performance conducting polymer hydrogel for all-hydrogel bioelectronic interfaces. *Nat Mater*. 2023;22:895–902.
[67] Choi G, Kim J, Kim H, et al. Motion-adaptive tessellated skin patches with switchable adhesion for wearable electronics. *Adv Mater*. 2025;37:e2412271.
[68] Wu X, Mori T. Sub-lattice amorphization as a new driver of room temperature plasticity in inorganic semiconductors. *Innovation (Cambridge (Mass.))*. 2025;6:100891.
[69] Zhong G, Liu Q, Wang Q, et al. Fully integrated microneedle biosensor array for wearable multiplexed fitness biomarkers monitoring. *Biosens Bioelectron*. 2024;265:116697.
[70] Wang S, Qiao Y, Liu X, et al. Reduced graphene oxides modified Bi2Te3 nanosheets for rapid photo-thermoelectric catalytic therapy of bacteria-infected wounds. *Adv Funct Mater*. 2022;33:2210098.
[71] Gao M, Luo Y, Zheng L, et al. Biomimetic electric interface-mediated cellular activation promotes diabetic wound healing via self-powered wearable thermoelectric patch. *Mater Today Bio*. 2025;35:102520.
[72] He J, Zhang W, Cui Y, et al. Multifunctional Cu_2Se/F127 Hydrogel with SOD-like enzyme activity for efficient wound healing. *Adv Healthcare Mater*. 2024;13:2303599.
[73] Zang Y, Zhang W, Wang P, et al. Bi_2Se_3/PAAS hydrogels with photothermal and antioxidant properties for bacterial infection wound therapy by improving vascular function and regulating glycolipid metabolism. *Adv Healthcare Mater*. 2025;14:2401810.
[74] Rahman S, Arif M, Khan SU, et al. Fabrication of new TiO_2-SnSe composites with enhanced antibacterial performance against E. coli and S. aureus. *Mater Today Commun*. 2024;39:108662.
[75] Song JH, Yoon T, Lee SM, et al. GeTe nanosheets as theranostic agents for multimodal imaging and therapy of inflammatory bowel disease. *Adv Funct Mater*. 2022;32:2107433.
[76] Li Y, Li X, Zhang S, et al. Autonomic self-healing of PEDOT: PSS achieved via polyethylene glycol addition. *Adv Funct Mater*. 2020;30:2002853.
[77] Rahmati M, Silva EA, Reseland JE, et al. Biological responses to physicochemical properties of biomaterial surface. *Chem Soc Rev*. 2020;49:5178–5224.
[78] Williams DF. On the mechanisms of biocompatibility. *Biomaterials*. 2008;29:2941–2953.
[79] Myllymaa S, Myllymaa K, Korhonen H, et al. Surface characterization and in vitro biocompatibility assessment of photosensitive polyimide films. *Colloids Surf B Biointerfaces*. 2010;76:505–511.
[80] Ma Y, Zhang DY, Peng Z, et al. Delivery of platinum (iv) prodrugs via Bi_2Te_3 nanoparticles for photothermal-chemotherapy and photothermal/photoacoustic imaging. *Mol Pharm*. 2020;17:3403–3411.
[81] Yazdimamaghani M, Razavi M, Mozafari M, et al. Biomineralization and biocompatibility studies of bone conductive scaffolds containing poly(3,4-ethylenedioxythiophene): poly(4-styrene sulfonate) (PEDOT: PSS). *J Mater Sci Mater Med*. 2015;26:274.
[82] Ren QW, Wang Y, Qian J, et al. Biosynthesis of Ag_2Se nanoparticles as a broad-spectrum antimicrobial agent with excellent biocompatibility. *J Hazard Mater*. 2023;465:133201.
[83] Kang MS, Kwon M, Jang HJ, et al. Biosafety of inorganic nanomaterials for theranostic applications. *Emergent Mat*. 2022;5:1995–2029.
[84] Wan M, Li T, Chen H, et al. Biosafety, functionalities, and applications of biomedical micro/nanomotors. *Angew Chem Int Ed*. 2020;60:13158–13176.
[85] Thanusha AV, Koul V. Biocompatibility evaluation for the developed hydrogel wound dressing - ISO-10993-11 standards -in vitroandin vivostudy. *Biomed Phys Eng Expr*. 2021;8:015010.
[86] Hong S, Gu Y, Seo JK, et al. Wearable thermoelectrics for personalized thermoregulation. *Sci Adv*. 2019;5:eaaw0536.
[87] Hou W, Nie X, Zhao W, et al. Fabrication and excellent performances of $Bi_{0.5}Sb_{1.5}Te_3$/epoxy flexible thermoelectric cooling devices. *Nano Energy*. 2018;50:766–776.
[88] Liu Y, Li Y, Wu M, et al. Nanoengineering approach toward high power factor Ag_2Se/Se composite films for flexible thermoelectric generators. *ACS Appl Mater Interfaces*. 2023;15:36587–36593.
[89] Wu H, Shi XL, Duan J, et al. Advances in Ag_2Se-based thermoelectrics from materials to applications. *Energy Environ Sci*. 2023;16:1870–1906.
[90] Wang J, Fan W, Yang J, et al. Tetragonal–orthorhombic–cubic phase transitions in Ag_2Se nanocrystals. *Chem Mater*. 2014;26:5647–5653.
[91] Lin S, Guo L, Wang X, et al. Revealing the promising near-room-temperature thermoelectric performance in Ag_2Se single crystals. *J Materiomics*. 2023;9:754–761.
[92] Yu H, Hu Z, He J, et al. Flexible temperature-pressure dual sensor based on 3D spiral thermoelectric Bi_2Te_3 films. *Nat Commun*. 2024;15:2521.
[93] Ma H, Pu S, Wu H, et al. Flexible Ag_2Se thermoelectric films enable the multifunctional thermal perception in electronic skins. *ACS Appl Mater Interfaces*. 2024;16:7453–7462.
[94] Li R, Ou W, Zhu J, et al. Exceptional thermoelectric and mechanical performance in $(Bi, Sb)_2Te_3$ matrix facilitated by $AgInSe_2$ alloying. *Chem Eng J*. 2024;497:154624.
[95] Zhu J, Tan X, Hong M, et al. Multiphase coherent nanointerface network enhances thermoelectric performance for efficient energy conversion and contactless thermosensation applications in GeTe. *Adv Energy Mater*. 2024;14:2402552.
[96] Wu J, Liu H, Chen W, et al. Device integration of electrochemical biosensors. *Nat Rev Bioeng*. 2023;1:346–360.
[97] Minopoli A, Della Ventura B, Lenyk B, et al. Ultrasensitive antibody-aptamer plasmonic biosensor for malaria biomarker detection in whole blood. *Nat Commun*. 2020;11:6134.
[98] Chang HJ, Zúñiga A, Conejero I, et al. Programmable receptors enable bacterial biosensors to detect pathological biomarkers in clinical samples. *Nat Commun*. 2021;12:5216.
[99] Ren X, Yang M, Yang T, et al. Highly conductive PPy–PEDOT: PSS hybrid hydrogel with superior biocompatibility for bioelectronics application. *ACS Appl Mater Interfaces*. 2021;13:25374–25382.
[100] Yang T, Yang M, Xu C, et al. PEDOT: PSS hydrogels with high conductivity and biocompatibility for in situ cell sensing. *J Mater Chem B*. 2023;11:3226–3235.
[101] Sultana N, Chang HC, Jefferson S, et al. Application of conductive poly(3,4-ethylenedioxythiophene): poly(styrenesulfonate) (PEDOT: PSS) polymers in potential biomedical engineering. *J Pharm Investig*. 2020;50:437–444.
[102] Balint R, Cassidy NJ, Cartmell SH. Conductive polymers: towards a smart biomaterial for tissue engineering. *Acta Biomater*. 2014;10:2341–2353.
[103] Tang L, Thevenot P, Hu W. Surface chemistry influences implant biocompatibility. *Curr Top Med Chem*. 2008;8:270–280.
[104] Moxon KA, Kalkhoran NM, Markert M, et al. Nanostructured surface modification of ceramic-based microelectrodes to enhance biocompatibility for a direct brain-machine interface. *IEEE Trans Biomed Eng*. 2004;51:881–889.
[105] Meyers SR, Grinstaff MW. Biocompatible and bioactive surface modifications for prolonged in vivo efficacy. *Chem Rev*. 2012;112:1615–1632.
[106] Stříteský S, Marková A, Víteček J, et al. Printing inks of electroactive polymer PEDOT: PSS: the study of biocompatibility, stability, and electrical properties. *J Biomed Mater Res A*. 2018;106:1121–1128.
[107] Cristaldi DA, Yanar F, Mosayyebi A, et al. Easy-to-perform and cost-effective fabrication of continuous-flow reactors and their application for nanomaterials synthesis. *N Biotechnol*. 2018;47:1–7.
[108] Metcalf CJE, Lessler J. Opportunities and challenges in modeling emerging infectious diseases. *Science*. 2017;357:149–152.
[109] Wang WX, Liu Y, Wang YX, et al. A novel and convenient preparation of antibacterial polyacrylonitrile nanofibers via post-modification using nitrile click chemistry and electrospinning. *Chem Pap*. 2017;72:191–200.
[110] Fan W, Zhang Y, Sun Y, et al. Durable antibacterial and temperature regulated core-spun yarns for textile health and comfort applications. *Chem Eng J*. 2023;455:140917.
[111] Alipuly M, Kanzhigitova D, Bexeitova A, et al. Stable conductive PANI-based hydrogels with antibacterial activity. *Adv Compos Hybrid Mater*. 2024;8:56.
[112] Barman SR, Chan SW, Kao FC, et al. A self-powered multifunctional dressing for active infection prevention and accelerated wound healing. *Sci Adv*. 2023;9:eadc8758.
[113] Koh TJ, DiPietro LA. Inflammation and wound healing: the role of the macrophage. *Expert Rev Mol Med*. 2011;13:e23.
[114] Stratford JP, Edwards CLA, Ghanshyam MJ, et al. Electrically induced bacterial membrane-potential dynamics correspond to cellular proliferation capacity. *Proc Natl Acad Sci USA*. 2019;116:9552–9557.
[115] Wu F, Zheng H, Wang W, et al. Rapid eradication of antibiotic-resistant bacteria and biofilms by MXene and near-infrared light through photothermal ablation. *Sci China Mater*. 2020;64:748–758.
[116] Zhou X, Yan Y, Lu X, et al. Routes for high-performance thermoelectric materials. *Mater Today*. 2018;21:974–988.

[117] Li JF, Liu WS, Zhao LD, et al. High-performance nanostructured thermoelectric materials. *NPG Asia Mater*. 2010;2:152–158.
[118] Yang L, Chen ZG, Dargusch MS, et al. High performance thermoelectric materials: progress and their applications. *Adv Energy Mater*. 2017;8:1701797.
[119] Mehdizadeh Dehkordi A, Zebarjadi M, He J, et al. Thermoelectric power factor: enhancement mechanisms and strategies for higher performance thermoelectric materials. *Mater Sci Eng R Rep*. 2015;97:1–22.
[120] Pei Y, Gibbs ZM, Gloskovskii A, et al. Optimum carrier concentration in n-type PbTe thermoelectrics. *Adv Energy Mater*. 2014;4:1400486.
[121] Dutková E, Kováč J, Kováč J, et al. Properties of mechanochemically synthesized famatinite Cu_3SbS_4 nanocrystals. *Micro*. 2023;3:458–470.
[122] Zhang L, Shi XL, Yang YL, et al. Flexible thermoelectric materials and devices: from materials to applications. *Mater Today*. 2021;46:62–108.
[123] Cheng J, Zhang J, Qiu P, et al. Preparation and thermoelectric transport properties of P-doped β-$FeSi_2$. J. *Inorg Mater*. 2024;39:895–902.
[124] Hou Z, Wang D, Hong T, et al. Boosting thermoelectric performance of n-type PbS through synergistically integrating In resonant level and Cu dynamic doping. *J Phys Chem Solids*. 2021;148:109640.
[125] Heremans JP, Wiendlocha B, Chamoire AM. Resonant levels in bulk thermoelectric semiconductors. *Energy Environ Sci*. 2011;5:5510–5530.
[126] Zebarjadi M, Esfarjani K, Dresselhaus MS, et al. Perspectives on thermoelectrics: from fundamentals to device applications. *Energy Environ Sci*. 2011;5:5147–5162.
[127] Pei Y, Wang H, Snyder GJ. Band engineering of thermoelectric materials. *Adv Mater*. 2012;24:6125–6135.
[128] Pei Y, Shi X, LaLonde A, et al. Convergence of electronic bands for high performance bulk thermoelectrics. *Nature*. 2011;473:66–69.
[129] Pei Y, Tan G, Feng D, et al. Integrating band structure engineering with all-scale hierarchical structuring for high thermoelectric performance in PbTe system. *Adv Energy Mater*. 2016;7:1601450.
[130] Zhao W, Wei P, Zhang Q, et al. Multi-localization transport behaviour in bulk thermoelectric materials. *Nat Commun*. 2015;6:6197.
[131] Zhao LD, Wu HJ, Hao SQ, et al. All-scale hierarchical thermoelectrics: MgTe in PbTe facilitates valence band convergence and suppresses bipolar thermal transport for high performance. *Energy Environ Sci*. 2013;6:3346–3355.
[132] Zhang LJ, Qin P, Han C, et al. Enhanced thermoelectric performance through synergy of resonance levels and valence band convergence via Q/In (Q = Mg, Ag, Bi) co-doping. *J Mater Chem A*. 2017;6:2507–2516.
[133] Jaworski CM, Kulbachinskii V, Heremans JP. Resonant level formed by tin in Bi_2Te_3 and the enhancement of room-temperature thermoelectric power. *Physi Rev B*. 2009;80:233201.
[134] Slyn'ko VE. On the resonant level of chromium in the rhombohedral and cubic phases of $Pb_{1-x-y}Ge_xCr_yTe$ alloys. *Semiconductors*. 2013;47:729–735.
[135] Zhu T, Liu Y, Fu C, et al. Compromise and synergy in high-efficiency thermoelectric materials. *Adv Mater*. 2017;29:1605884.
[136] Wang H, LaLonde AD, Pei Y, et al. The criteria for beneficial disorder in thermoelectric solid solutions. *Adv Funct Mater*. 2012;23:1586–1596.
[137] Qin YX, Xiao Y, Zhao LD. Carrier mobility does matter for enhancing thermoelectric performance. *APL Mater*. 2020;8:010901.
[138] Pei YL, Wu HJ, Wu D, et al. High thermoelectric performance realized in a BiCuSeO system by improving carrier mobility through 3d modulation doping. *J Am Chem Soc*. 2014;136:13902–13908.
[139] Zebarjadi M, Joshi G, Zhu G, et al. Power factor enhancement by modulation doping in bulk nanocomposites. *Nano Lett*. 2011;11:2225–2230.
[140] Yu B, Zebarjadi M, Wang H, et al. Enhancement of thermoelectric properties by modulation-doping in silicon germanium alloy nanocomposites. *Nano Lett*. 2012;12:2077–2082.
[141] Tsukazaki A, Akasaka S, Nakahara K, et al. Observation of the fractional quantum Hall effect in an oxide. *Nat Mater*. 2010;9:889–893.
[142] Li W, Zheng L, Ge B, et al. Promoting SnTe as an Eco-friendly solution for p-PbTe thermoelectric via band convergence and interstitial defects. *Adv Mater*. 2017;29:1605887.
[143] Biswas K, He J, Blum ID, et al. High-performance bulk thermoelectrics with all-scale hierarchical architectures. *Nature*. 2012;489:414–418.
[144] Fu C, Zhu T, Liu Y, et al. Band engineering of high performance p-type FeNbSb based half-Heusler thermoelectric materials for figure of merit zT > 1. *Energy Environ Sci*. 2014;8:216–220.
[145] Chen Z, Jian Z, Li W, et al. Lattice dislocations enhancing thermoelectric PbTe in addition to band convergence. *Adv Mater*. 2017;29:1606768.
[146] Kim SI, Lee KH, Mun HA, et al. Dense dislocation arrays embedded in grain boundaries for high-performance bulk thermoelectrics. *Science*. 2015;348:109–114.
[147] Zhu J, Shen X, Ding J, et al. Revealing the phonon properties for thermoelectric materials by neutron scattering. *Innov Ene*. 2024;1:100049.
[148] Lin YB, Feng TX, Qiong Q, et al. Preparation and thermal transport properties of $CoSb_3$ nano-compounds. *Acta Phys Sin*. 2004;53:3130–3135.
[149] Pohl RO. Lattice vibrations of glasses. *J Non-Cryst Solids*. 2006;352:3363–3367.
[150] Wei P, Yang J, Guo L, et al. Minimum thermal conductivity in weak topological insulators with bismuth-based stack structure. *Adv Funct Mater*. 2016;26:5360–5367.
[151] Toriyama MY, Brod MK, Gomes LC, et al. Tuning valley degeneracy with band inversion. *J Mater Chem A*. 2022;10:1588–1595.
[152] Toriyama MY, Snyder GJ. Band inversion-driven warping and high valley degeneracy. *Cell Rep Phy Sci*. 2023;4:101392.
[153] Wu CF, Wei TR, Li JF. Electrical and thermal transport properties of $Pb_{1-x}Sn_xSe$ solid solution thermoelectric materials. *Phys Chem Chem Phys*. 2015;17:13006–13012.
[154] Toriyama MY, Snyder GJ. Topological insulators for thermoelectrics: a perspective from beneath the surface. *Innovation (Camb)*. 2025;6:100782.
[155] Ma X, Lin C, Yang H, et al. Elevating thermoelectric performance in the sub-ambient temperature range for electronic refrigeration. *Innovation (Camb)*. 2025;6:100864.
[156] Mao J, Zhu H, Ding Z, et al. High thermoelectric cooling performance of n-type Mg_3Bi_2-based materials. *Science*. 2019;365:495–498.
[157] Pan Y, Yao M, Hong X, et al. $Mg_3(Bi, Sb)_2$ single crystals towards high thermoelectric performance. *Energy Environ Sci*. 2020;13:1717–1724.
[158] Imasato K, Kang SD, Snyder GJ. Exceptional thermoelectric performance in $Mg_3Sb_{0.6}Bi_{1.4}$ for low-grade waste heat recovery. *Energy Environ Sci*. 2019;12:965–971.
[159] Zhou L, Ma G-X, Tian W-X, et al. Chemically engineered hydroxyl-terminated polybutadiene yields stable and high-strain intrinsically conductive polyurethane piezoresistive sensors. *Chin J Polym Sci*. 2026;44:100–115.
[160] Zhang J, Song L, Sist M, et al. Chemical bonding origin of the unexpected isotropic physical properties in thermoelectric Mg_3Sb_2 and related materials. *Nat Commun*. 2018;9:4716.
[161] Liu J, Li A, Fu C, et al. Band anisotropy in thermoelectric materials. *Innov Mater*. 2023;1:100004.
[162] Chen N, Zhu H, Li G, et al. Improved figure of merit (z) at low temperatures for superior thermoelectric cooling in Mg3(Bi, Sb)2. *Nat Commun*. 2023;14:4932.
[163] Han Z, Li JW, Jiang F, et al. Room-temperature thermoelectric materials: challenges and a new paradigm. *J Materiomics*. 2021;8:427–436.
[164] Jia S, Ma H, Gao S, et al. Thermoelectric materials and devices for advanced biomedical applications. *Small*. 2024;20:2405019.
[165] Yuan X, Shi J, Kang Y, et al. Piezoelectricity, pyroelectricity, and ferroelectricity in biomaterials and biomedical applications. *Adv Mater*. 2023;36:2308726.
[166] Yin Y, Lin S, Xu Z, et al. Giant-thermopower ionogels for multifunctional energy harvesting through molecularly selective ionic pairing and hydrogen bonding. *Innov Ene*. 2024;1:100048.
[167] Yao S, Wei Y, Lu Z, et al. Review of research progress on concentrated solar energy utilization system. *Renewables*. 2023;1:397–414.
[168] Yun JS, Choi S, Im SH. Advances in carbon-based thermoelectric materials for high-performance, flexible thermoelectric devices. *Carbon Ene*. 2021;3:667–708.
[169] Yu H, Liu M, Lu X, et al. A cooling wound dressing for accelerating healing under sunlight. *Innovation (Camb)*. 2024;5:100670.
[170] Ahmad U, Hanaffi WNW, Islam A, et al. Cutting edge strategies for diabetic wound care: nanotechnology, bioengineering, and beyond. *BMEMat*. 2025;n/a:e70033.
[171] Ao H, Wang D, Ma L, et al. Copper-doped borosilicate bioactive glass coating modified bacterial cellulose functional dressing for diabetic ulcer. *BMEMat*. 2025;n/a:e70042.
[172] Gao Y, Chen X, He C, et al. Stimulus-responsive hydrogels for diabetic wound management via microenvironment modulation. *Biomater Sci*. 2025;13:3192–3212.

How to cite this article: Zhang Y, Hao Z, Li Z, Mu Y, Meng Z, Lian H. Thermoelectric materials for skin wound healing. MedMat 2026;3(2):e00040. doi: 10.1097/mm9.0000000000000040